Elucidation of the Role of miR-575 in Tumor Progression in Glioblastoma

Undergraduate Research Thesis

Presented in Partial Fulfillment of the Requirements for graduation “with Honors Research Distinction in Neuroscience” in the undergraduate colleges of The Ohio State University

by
Ashley Gray

The Ohio State University
March 2018

Project Advisor: Dr. Arnab Chakravarti, Department of Radiation Oncology

Table of Contents

Abstract	2
Relevance	4
Aims	6
Introduction	7
Materials and Methods	24
Results	31
Discussion	50
Conclusion	56
Acknowledgements	57
References	58

Abstract

Background: Glioblastoma (GBM) patients currently face poor survival outcomes with an average survival rate less than 15 months with treatment (radiation and temozolomide), while only 3-5% of patients survive more than 36 months (1). Although the mechanisms underlying tumor development and progression are still being elucidated, microRNAs (miRNAs) are promising candidates to explore as novel biomarkers and therapeutic targets in GBM due to their size, stability, and myriad of target genes (2). Previously, in a univariable analysis, our lab showed that higher levels of miR-575 were significantly associated with worse overall survival in GBM patients (HR: 1.3; p-value: 5.77E-05; FDR p-value: 0.0036). Additionally, miR-575 was found to be significantly associated with worse overall survival independent of age, gender, treatment and KPS (Karnofsky's Performance Status) in a multivariable analysis (HR: 1.2; p: 0.012; 95% CI (1.04-1.4)). Based on this preliminary finding, we hypothesized that miR-575 acts as an oncogene in GBM.

Methods: Cell proliferation, colony formation, and migration assays were performed to investigate the physiological role of miR-575 in GBM cell lines. qPCR, immunoblots, and luciferase assays were performed to validate the downstream targets of miR-575, determined by *in silico* database analyses. Clonogenic assays and cell viability assays were then used to assess the effect of miR-575 on radiosensitivity and chemosensitivity, respectively.

Results: Overexpression of miR-575 significantly increased cell proliferation and cell motility in different GBM cell lines *in vitro*. *p27/CDKN1B* and *BLID/BRCC2*, both tumor-suppressor genes, were identified as putative targets of miR-575 and their expression

was inversely correlated with miR-575 *in vitro*. No clear effect of miR-575 was observed on radiosensitivity and chemosensitivity.

Conclusion: Our results suggest that miR-575 may serve as a novel prognostic biomarker in GBM, with higher expression correlating with worse overall survival. miR-575 likely acts as an oncogene by targeting tumor-suppressor genes *p27* and *BLID*. Knowledge of the role of miR-575 in tumor progression as well its underlying mechanisms may improve determination of prognosis and treatment response in GBM. Future work will focus on validating miR-575 as a prognostic biomarker in an independent GBM cohort. The physiological study of miR-575 should be replicated in primary glioma cell lines prior to *in vivo* experiments. Furthermore, additional target genes were identified during *in silico* analyses that should be investigated for further elucidation of the mechanisms underlying the oncogenic effect of miR-575 in GBM.

Relevance

Under the current treatment regimens, including surgical resection, chemotherapy, and radiation therapy, median overall survival times remain poor for GBM patients. Novel therapeutic approaches are desperately needed for survival and quality of life improvements in GBM patients. Due to heterogeneity in GBM, tumors within the same histological category demonstrate variations in prognoses and responses, although collectively GBMs result in poor clinical outcomes. (3). Therefore, identification of novel biomarkers is necessary in order to molecularly characterize these tumors, rather than pathologically, so that more personalized, effective treatments can be delivered. While biomarkers are already being utilized in GBM, such as MGMT methylation status, a multi-faceted approach from proteomics, genomics, and epigenetics will improve the effectiveness of the current classification system in the temozolomide era (4).

miRNAs are ideal biomarker candidates due their stability in formalin-fixed paraffin embedded (FFPE) tissue and biofluids, as well as the affordability of their assays. Biologically, miRNAs are also exciting therapeutic candidates as they are capable of having a more global effect due to their myriad of target genes, many of which are oncogenes and tumor-suppressor genes. Dysregulated miRNAs are known to contribute to tumor progression in cancers through cell cycle, apoptosis, invasion, and cell metabolism (2). Therefore, elucidation of the mechanisms by which miRNAs regulate tumor development and progression is essential to better understand the pathogenesis of GBM.

The identification of significant miRNAs in GBM has the potential to improve overall survival of patients through more accurate risk classification, and with a better

understanding of the underlying biology of GBM, novel therapies will be developed and implemented in the clinic. Additionally, the relevance of this miRNA study extends beyond GBM, for significant microRNAs are often implicated in multiple cancers (2).

Aims

The aims of this project are to validate the biological significance of miR-575 *in vitro* using GBM cell lines and determine whether these findings have the potential to impact prognosis, treatment response, or novel therapeutic approaches in glioblastoma.

Aim 1: Validate the physiological role of miR-575 in GBM and underlying mechanisms *in vitro*. Based on clinical data showing that higher miR-575 expression levels were associated with worse overall survival, GBM cell lines will be used to assess effects of miR-575 on aspects of tumor progression and to determine its target genes. We hypothesize that miR-575 will have an oncogenic effect in GBM by down-regulating tumor suppressor genes.

Aim 2: Determine the effect of miR-575 on therapeutic sensitivity. miR-575 expression levels will be assessed in GBM cell lines treated with either temozolomide or radiation therapy. We hypothesize that miR-575 expression might predict response in both temozolomide and radiation therapy due to its correlation with worse overall survival in our GBM patient cohort.

Introduction

1. Glioblastoma

1.1 Background

Glioblastoma (GBM) is the most aggressive brain tumor, a grade IV glioma, with an average survival rate of 15 months with standard treatment (3). The incidence of GBM in the U.S. is 2-3 per 100,000 (5). GBM is typically detected using magnetic resonance imaging (MRI), and if possible, surgical resection is done first to remove the majority of the tumor and biopsy the tumor for diagnosis. GBM is assessed histologically by the WHO guidelines, based on necrosis and microvascular proliferation (6). Currently, GBM is treated according to the Stupp protocol, which includes radiotherapy plus concomitant and adjuvant temozolomide (TMZ).

Differences in survival times indicate that a subset of patients may have molecular features that produce more favorable outcomes. This underlying heterogeneity warrants the use of molecular biomarkers to better stratify patients for treatment and determine prognosis (4, 7-9). Some molecular biomarkers are currently assessed at diagnosis in GBM, including isocitrate hydrogenase (*IDH*), O6-methylguanine-DNA-methyltransferase (*MGMT*) methylation, and *ATRX* status (6).

1.2 Classification

The 2016 World Health Organization (WHO) Classification of Gliomas proposes that glioblastomas should be classified both histologically and genetically in order to improve prognostic outcomes and treatment responses. This was the first time that molecular markers were incorporated into the diagnosis of brain tumors. Diffuse glioma classification now separates astrocytomas and glioblastomas based on the presence of *IDH1/2* gene

mutations. Additionally, the 1p/19q codeletion is now required for oligodendroglioma diagnosis in addition to the *IDH1/2* gene mutation (10).

Importantly, glioblastomas are classified as either primary or secondary tumors. 90% of GBMs are primary or *de novo*, meaning that the tumor developed rapidly without evidence of precursor lesions. In contrast, secondary GBM is a progression of a less malignant tumor, usually a diffuse or anaplastic astrocytoma (9). Additionally, secondary GBMs tend to yield more favorable outcomes. While primary and secondary GBMs are histologically similar, important genetic and epigenetic differences distinguish the subtypes. Overall, secondary GBMs are more genetically homogenous, while primary GBMs express greater heterogeneity (9).

GBMs are further classified based upon cDNA expression profiles as either proneural, neural, classical, or mesenchymal. These subtypes are defined by the tumor's precursor cell type and further classified by genetic differences (9, 11, 12). Different subtypes of GBM have been shown to respond differently to treatment, temozolomide and radiation therapy. Thus, it is crucial to further define these subtypes using molecular markers. Additionally, molecular markers aid in understanding GBM pathogenesis, which can provide key insight into more efficacious interventions (11).

1.3 Notable Genetic Alterations

Genetic alterations of GBM are summarized in Figure 1. Primary and secondary GBM possess key genetic differences. In primary GBM, *EGFR* is amplified, *PTEN* is often mutated, and chromosome 10q is lost. In contrast, *TP53* is typically mutated and chromosome 19q is lost in secondary GBM (9, 11).

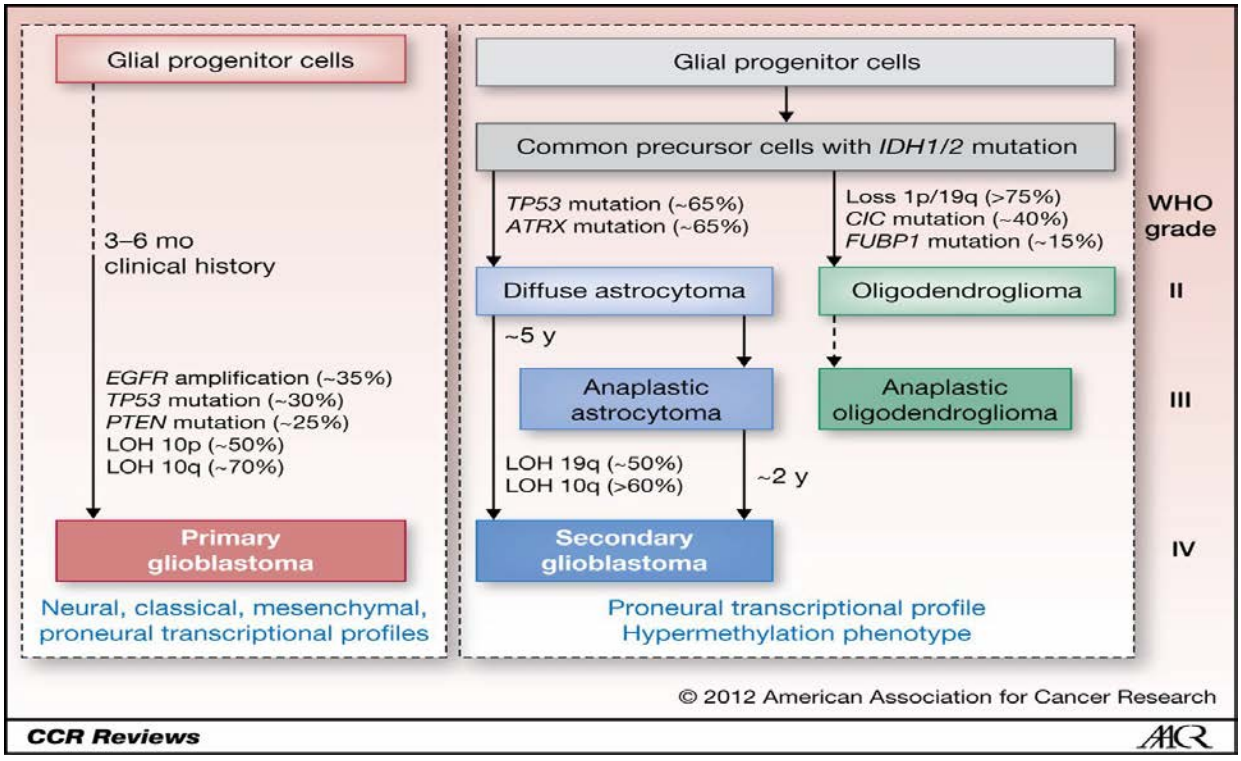

Figure 1: Genetic alterations differentiate primary and secondary glioblastoma and contribute to disease progression (http://clincancerres.aacrjournals.org).

However, *IDH1* has emerged as the main gene to differentiate the two subtypes. Less than 10% of primary GBMs have *IDH* mutations. In contrast, over 80% of secondary GBMs have *IDH1* mutations (13). In primary GBM, *IDH1/2* mutations actually yield more favorable outcomes than *IDH1/2* wildtype. GBM patients with *IDH1/2* mutations have an average survival of 31 months, while *IDH1/2* wildtype patients have an average survival of 15 months (13). While this mechanism remains unclear, one possibility is that this could

be due to decreased migratory ability in the mutant tumors, or a negative effect on the tumor posed by 2HG production (13). Interestingly, *IDH1* mutations are relied upon more heavily for diagnosis than histological observation; this is yet another instance of the significance of genetic alterations in GBM (9). More biomarkers are necessary to further identify GBM subtype and increase our understanding of the mechanisms underlying tumor progression.

1.4 Biomarkers in GBM

While *IDH1/2* mutations permit the molecular classification of GBMs, biomarkers can also predict treatment response. Notably, biomarkers like *MGMT* promoter methylation status indicate differential survival times and response to chemotherapy. Patients with *MGMT* promoter hypermethylation experience longer survival times due to the effect of MGMT on temozolomide treatment (14). Temozolomide acts by methylating DNA, which is prevented when *MGMT* is methylated resulting in reduced MGMT protein levels. While MGMT in its active form can reverse the TMZ-induced alkylated bases, *MGMT* methylation reverses this process by depleting MGMT protein levels. Thus, methylation allows temozolomide to cause a greater number of cells to undergo apoptosis, which leads to more favorable patient outcomes (14). More molecular biomarkers beyond MGMT, including miRNA signatures, will help to further stratify patients into more specific and accurate groups, which will ultimately improve clinical decision-making (3, 8).

2. microRNAs as biomarkers in GBM

2.21 miRNA Biogenesis

Recently, miRNAs have emerged as promising and novel candidates for GBM biomarkers. miRNAs are small non-coding RNAs, about 22 nucleotides (nt) in length, that can lead to mRNA degradation or translational repression. miRNAs are often formed in areas of relaxed chromatin, known as euchromatin, which is often hypomethylated. In contrast, hypermethylated, tightly wound regions of chromatin, known as heterochromatin, are less likely to facilitate miRNA formation (2). In the nucleus, primary miRNA (pri-miRNA) is first transcribed by RNA polymerase II, as shown in Figure 1. Pri-miRNA then forms a hairpin loop shape and is capped and polyadenylated. Pri-miRNA is then cleaved by an RNAse endonuclease III called DROSHA and DiGeorge syndrome critical region gene 8 (DGCR8), into pre-miRNA of approximately 70 nt. This pre-miRNA is then transported into the cytoplasm via Exportin-5, which is a double-stranded binding protein. In the

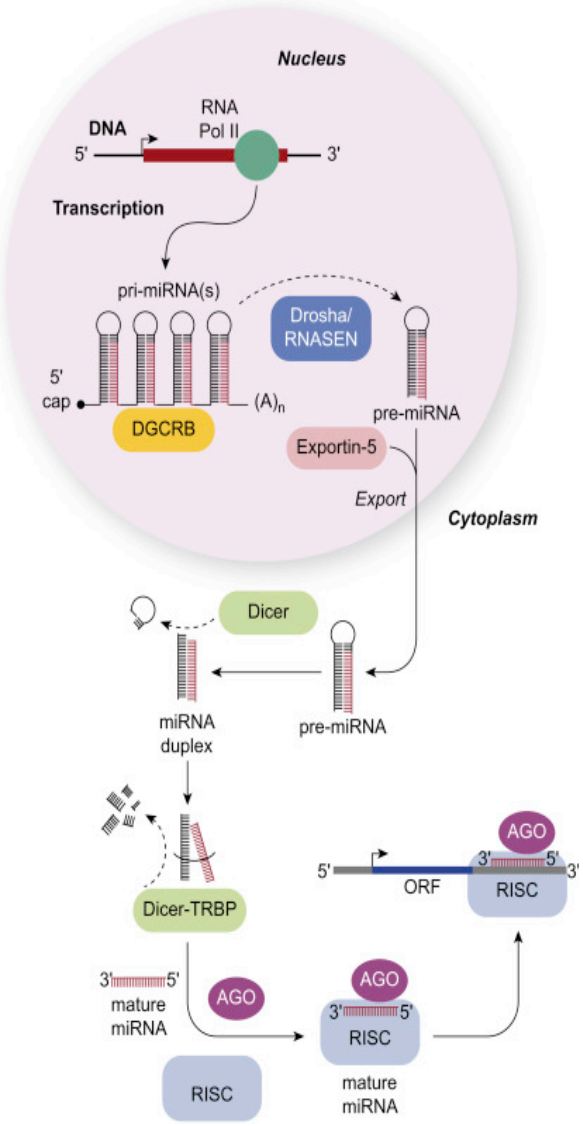

Figure 2: miRNA processing begins in the nucleus and ends in the cytoplasm. The enzymes RNA Pol II, DGCR8, DROSHA, Exportin-5, Dicer, AGO, and RISC are shown, respectively. Biogenesis results in a mature miRNA that can bind the 3'UTR of complementary mRNA (2).

cytoplasm, miRNA binds to the RNAse III endonuclease enzyme Dicer where it is cleaved into a mature, double-stranded RNA of approximately 22 bp (2, 7). One strand of the mature miRNA, known as the guide strand, is now free to bind an Argonaute (AGO) protein in the RNA Silence-Inducing Complex (RISC). The strand of the miRNA duplex chosen as the guide strand is thought to be the strand with the less tightly bound 5' end. Helicase samples both 5' ends and begins unwinding the easier of the two. This miRNA bound to RISC may now bind to complementary sequences, most commonly in the 3'UTR of target mRNAs (15).

2.22 miRNA targeting

Once bound to mRNA, miRNA may either cleave mRNA or block translation without cleavage. High complementarity between miRNA and mRNA typically leads to cleavage and subsequent degradation (16). Cleavage occurs at the 10^{th} or 11^{th} nucleotide, regardless or complementarity. However, low complementarity facilitates translational blockage without cleaving mRNA. This phenomenon is exhibited in Figure 3. miRNA will remain intact after mRNA cleavage. In fact, miRNA is more stable than RNA in adverse conditions. miRNA can be packaged extracellularly and is usually bound to an RNA-binding protein or a lipoprotein complex (7, 15).

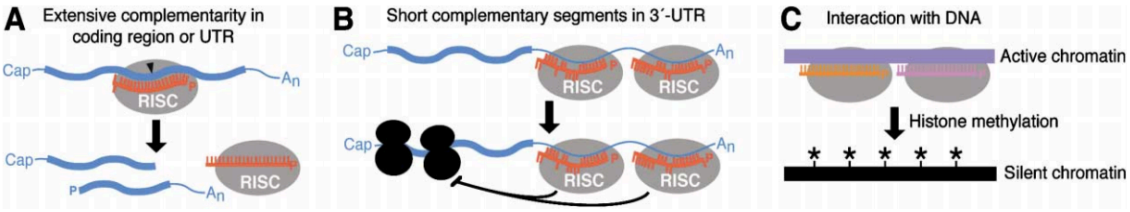

Figure 3. The Actions of Small Silencing RNAs
(A) Messenger RNA cleavage specified by a miRNA or siRNA. Black arrowhead indicates site of cleavage.
(B) Translational repression specified by miRNAs or siRNAs.
(C) Transcriptional silencing, thought to be specified by heterochromatic siRNAs.

Figure 3: Small silencing RNAs, either miRNAs or siRNAs, can act in several distinct mechanisms depending on complementarity with mRNA. miRNAs can act via cleavage (A), translation repression (B), or transcriptional silencing (C) (16).

2.23 Benefits and limitations of miRNAs in the clinic

In the past decade, numerous studies have noted the relevance of aberrant miRNA expression in cancer due to their ability to promote angiogenesis, invasion, and metastasis through control of oncogenes and tumor-suppressor genes (16). miRNAs help to further elucidate oncogenic pathways, which provide additional gene targets for therapeutic innovation. Individual miRNAs and miRNA expression profiles are now being studied for their uses in diagnosis, prognosis, and therapeutics. (17). While many studies have highlighted the exciting potential of miRs as biomarkers and therapeutic agents, several obstacles must be overcome before miRs can be effectively implemented in the clinic for GBM.

Traditional methodologies of cancer diagnosis involve histological classification following biopsy. Since miRNAs are readily found in the blood and urine, miRNA analyses can be performed non-invasively and inexpensively (2). The novelty of using microRNAs as biomarkers lies in their high intrinsic stability in the bloodstream and cerebrospinal fluid (CSF). MiRNAs are more stable than their RNA counterpart in relatively hot or acidic

conditions making them more amenable to FFPE-based assays. Additionally, miRNAs have a very low molecular weight, which makes them good candidates for delivery in therapeutics (2). MicroRNAs would allow for non-invasive diagnosis and serve as indicators of prognosis and treatment response (2, 7, 8). Individual miRNAs and miRNA expression profiles are associated with survival patterns in GBM. Current miRNA reviews indicate that the ideal use of miRNAs as biomarkers lies in signatures consisting of multiple microRNAs that are differentially expressed in GBM compared to normal tissues and distinct from other cancers (8). Additionally, microRNAs can be used to distinguish between GBM subclasses (8, 12). A recent study used 261 microRNAs to distinguish five subclasses of glioblastoma and have reported that microRNAs enhance the ability to distinguish between different classes of GBM both histologically and prognostically (12).

Currently, studies involving miRNAs are highly variable, meaning that a double-headed approach utilizing bioinformatics and molecular studies is necessary (8). For use as a gene therapy, miRNAs are exciting candidates as they are capable of having a more global effect due to their myriad of target genes, many of which are oncogenes and tumor-suppressor genes.

While the risks of using miRNAs as biomarkers are minimal, the use of miRNAs as therapies could cause off-target effects and toxicity to the patient (7, 8). There are additional limitations to consider when proposing miRNAs as therapeutic agents. Specifically for gliomas, there could be additional challenges in delivery due to the highly selective blood-brain barrier. Lastly, even once the miRNA is the brain, it may be another challenge to get the miRNA inside the cell due to high interstitial pressure of tumor cells (7).

Additional concerns surround the validity of miRNAs as biomarkers. While several miRNAs maintain consistent expression, there are inconsistent data regarding miRNA expression between GBM tissue and serum (8). Furthermore, miRNA expression profiles obtained from serum could eventually help distinguish cancer types without biopsy (8).

2.24 miRNA in clinical trials

While there are no current miRNA clinical trials in glioma, miRNA therapies have reached clinical trials in other cancers and diseases (18-20). The first microRNA to reach a Phase II clinical trial was antimiR-122 for treatment of hepatitis C virus infection (18). The study of the antisense oligonucleotide would be used in conjunction with other current therapies. Specifically in cancer, two miRs have recently reached Phase III clinical trials. MiR-34 (MRX34) was the first miRNA to reach Phase I clinical trial for patients with liver cancer. However, the study was terminated in 2016 after five adverse immune responses occurred (21). Another study completed in 2017 utilized *EGFR*-targeted miR-16-based miRNA for treatment in pleural mesothelioma and non-small cell lung cancer. While the results of this study have not yet been published, this miRNA therapy did pass initial safety trials (19).

2.25 Delivery Systems

MicroRNA mimics and anti-miRs are used for transfection into mammalian cell lines for physiological and therapeutic studies *in vitro*. They also serve as potential therapeutic strategies *in vivo*. Anti-miRs are single stranded miRNA passenger strands that bind to the active miRNA strand, which is now left unable to be processed by RISC. In contrast, mimics act as endogenous double-stranded miRNAs. Both are low molecular weight oligonucleotides (2, 7). Both mimics and anti-miRs would need to be chemically

modified prior to delivery to avoid degradation by nucleases. Figure 4 shows the action of both miRNA mimics and anti-miRs with target mRNA.

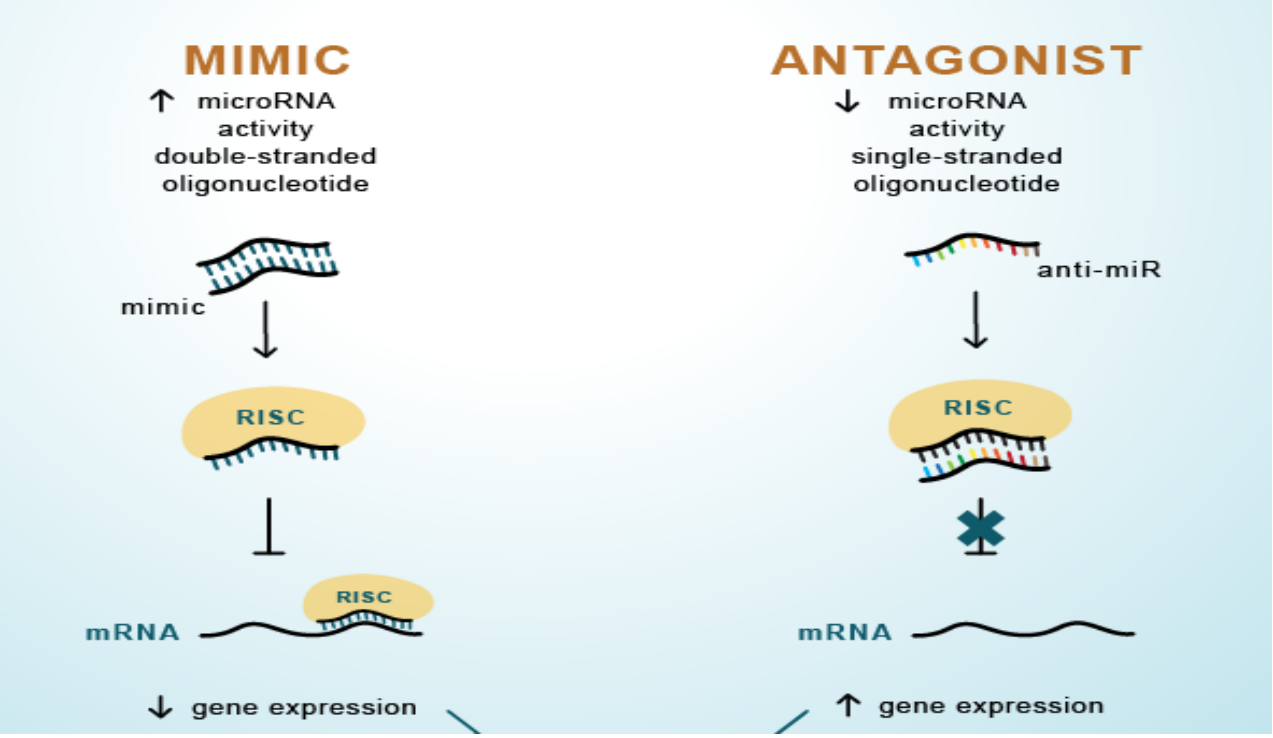

Figure 4: Mimic and antagonist structure and effect on microRNA activity and subsequent gene expression (http://www.aptamir.com).

Other therapeutic opportunities for miRNA include miRNA masks and miRNA sponges. miRNA masks are single-stranded and bind perfectly to the miRNA's target in mRNA 3'UTR. In this therapy, miRNA is not degraded, so off target effects are diminished. On the other hand, miRNA sponges include multiple sites for miRNA binding and sequester it away from the target gene (7).

For delivery of this miRNA replenishment and inhibition molecules, lentiviruses, adenoviruses, or nanoparticles may serve as promising options.

3. Validating miRNAs in GBM

3.1 Identifying clinically relevant miRNAs

If miRNAs are implemented in the clinic, there are several options for detection in patient serum. Likely techniques that would be used to detect miRNAs would be Nanostring, microarray, next generation RNA sequencing (NGS), and RT-qPCR. Microarrays can detect a more widespread effect, however, RT-qPCR is much more specific and is recommended for diagnostic purposes (8).

In this study, and in other clinical studies, Nanostring was utilized for widespread detection of miRNA in FFPE samples. However, for detection of miRNA expression levels within the laboratory, RT-qPCR techniques are more commonly used due to its robustness, cost-effectiveness, and routine use.

3.2 Aspects of tumorigenesis affected by miRNAs

In order to validate a microRNA *in vitro* for GBM, its physiological effect on tumorigenesis must be elucidated. miRNAs can target pathways in many aspects of tumorigenesis, but miRNAs are known to be implicated in angiogenesis, invasion, and cell metabolism.

Angiogenesis occurs in order to navigate more oxygenated blood to the tumor site. In a growing tumor, oxygen is used readily resulting in a hypoxic environment. The tumor must obtain more oxygen through increased availability of oxygenated blood. The mechanism of angiogenesis involves the release of pro-angiogeneic factors like vascular endothelial growth factor (VEGF) to increase blood vessel formation. However, during this rapid formation of blood vessels, inadequate formation occurs resulting in leaky blood vessels (8). These leaky blood vessels actually prevent the effective delivery of oxygen to the tumor site. In addition to oxygen, chemotherapy also cannot effectively reach the tumor site, which promotes treatment resistance (2, 7). Angiogenesis is a key component

of tumorigenesis that is targeted frequently in GBM due to its role in treatment resistance. Combatting angiogenesis may be an effective strategy for therapeutic intervention.

Both miR-7 and miR-296 are implicated in glioma angiogenesis. Down-regulation of miR-7 inhibits angiogenesis, while up-regulation of miR-296 promotes angiogenesis (22, 23). miR-296 acts by targeting hepatocyte growth factor-regulated tyrosine kinase substrate (HGS) which degrades VEGFRs and promotes angiogenesis (7). miR-7 acts through the EGFR and PI-3K signaling pathways (7).

Glioblastomas are highly invasive and infiltrate other neurons and glia, rather than metastasizing to other areas of the body. Due a high number of invasive cells, surgical resection and treatment delivery become increasingly difficult (7). Invasion occurs when GBM cells acquire a mesenchymal phenotype and migrate along blood vessels. The cells then extend from the extracellular matrix and spread to the parenchyma. Matrix metalloproteinases (MMPs) and uro-kinase type plasminogen activator (uPA) are also prominent factors in physiological invasiveness in GBM that act by degrading the extracellular matrix and promoting tumor invasion (ECM) (24). Another significant protein pathway in this mechanism is the hepatocyte growth factor (HGF) and its receptor c-MET (7). Interestingly, Bell et al. reported that increased levels of c-MET are associated with worse overall survival in GBM (4).

Additionally, radiation therapy is known to increase the invasiveness of GBM cells. Increased invasion is observed following radiation therapy, which exhibits morphology distinct from physiological invasion (24). This impacts the efficacy of subsequent radiation as tumor cells have migrated outside the geographic field of radiation (24). The mechanism underlying radiation-induced invasion involves the *EGFR/IGFR-1/PI-3K/Rho*

signaling pathway, whose activation promotes invasion (24). These mechanisms serve as crucial targets for reduced invasion in GBM and improved treatment outcomes.

miR-21, the first miR to be discovered in GBM, is up-regulated in GBM and contributes to invasion through down-regulation of MMP inhibitors (25). miR-10b is also up-regulated in GBM and promotes invasion through a mechanism involving *RhoC* and *uPAR* (7). The combination of these miRs has been suggested to be a valuable diagnostic tool in GBM when patients are treated with bevacizumab (BVZ), an alternate chemotherapy drug (8).

Lastly, cell metabolism plays a major role in tumor formation, especially in gliomas (7). While we are not clear whether cell metabolism is a result or a cause of tumor formation, metabolic alterations are present in many cancer types including glioblastoma (13). Cancer cells, in general, prefer aerobic glycolysis that converts glucose to lactate instead of pyruvate to bypass traditional oxidative phosphorylation for ATP production. This process is known as the Warburg Effect (13). Lactate is used as carbon source for cell proliferation, as normal cells engage in aerobic glycolysis in times of increased proliferative activity (13). Mutations of isocitrate hydrogenase 1 or 2 (*IDH1/2*), have been shown to disrupt cell metabolism and are believed to be involved in carcinogenesis. Mutations in *IDH1/2* lead to high levels of 2-hydroxyglutarate, which is thought to be an oncometabolite (13). *IDH1/2* also play a key role in producing NADPH, a premier reducing agent outside the mitochondria. NADPH also protects against radiation and oxidative stress.

Notably, miR-153 is known to act as a tumor suppressor by promoting apoptosis, but it may also function through targeting of glutaminase, which prevents the cell from obtaining energy through glutamine and thereby prevents proliferation (7).

4. miR-575

4.1 Univariable and Multivariable Analysis of miR-575 *on overall survival (OS) in GBM*

To generate miRNA expression data, a total of 268 FFPE tumor samples were provided from patients with newly diagnosed primary GBM (IDH-wild-type). These patients underwent biopsy or resection at the University of Utrecht, Netherlands from 2005 to 2014. Total RNA was isolated from these samples and used for further analyses. This study was approved by both University Medical Center Utrecht and The Ohio State University institutional review boards with waived patient consent due to the archival nature of the study.

miRNA expression data was analyzed using the NanoString human v3 array developed by NanoString Technologies (Seattle, WA). Total RNA was used from 268 tumor samples. Nanostring includes 798 miRNA probes, but miRs were filtered from this analysis if greater than 80% of the samples were missing the miR. MiR-575 was highlighted as one of the top miRNAs associated with overall survival in this cohort using univariable analysis (HR: 1.3; p-value: 5.77E-05; FDR p-value: 0.0036). Figure 5 shows a Kaplan-Meier Survival Analysis of miR-575 expression with overall survival in this GBM patient cohort (HR: 1.5; log-rank p-value: 0.004).

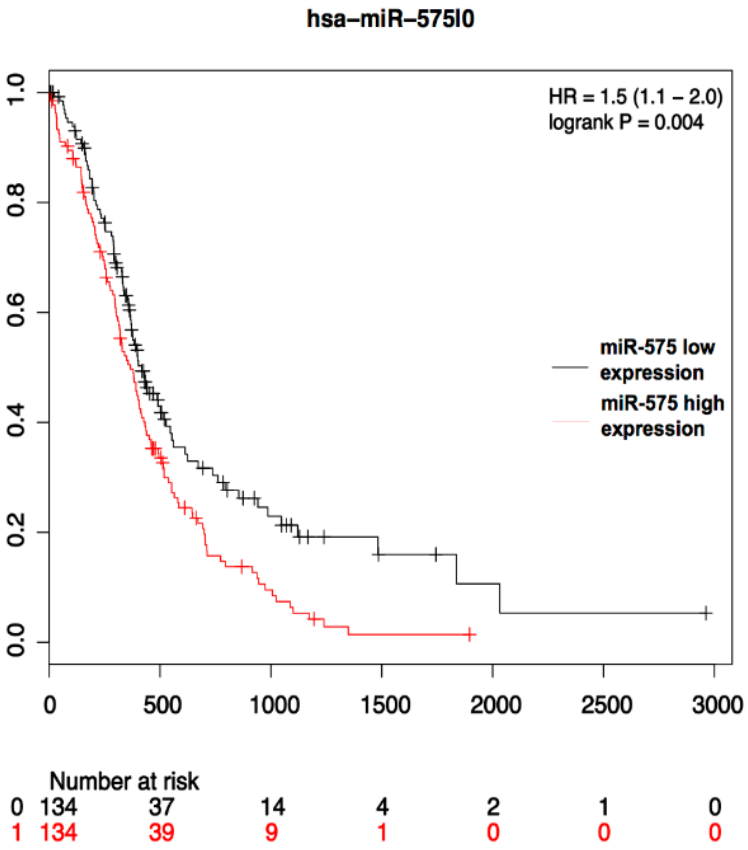

Figure 5: Correlation between miR-575 expression and overall survival by Kaplan-Meier analysis of GBM patients with high (n=134) and low (n=134) expression of miR-575 (HR: 1.3; p-value: 5.77E-05; FDR p-value: 0.0036).

In the multivariable analysis, miR-575 expression was assessed in the Utrecht patient cohort previously described (n=204). The sample size for the multivariable analysis is reduced compared to the univariable analysis because patients were excluded if they did not have information for all covariables. Table 1 shows multivariate statistical analysis of miR-575 expression in GBM patients based on age, treatment, gender, and all variables combined. As shown, miR-575 is a prognostic biomarker, which is independent of clinical variables in GBM (p: 0.012; HR: 1.21, 95% CI (1.04-1.4)). However, Table 2 shows that miR-575 expression level was not significant in a multivariable analysis when *MGMT* methylation status was included (p: 0.323; HR: 1.1;

95% CI (0.912-1.32)). This result suggests that the clinical utility of miR-575 is limited, since MGMT methylation is already used as a prognostic biomarker in GBM.

Table 1 Multivariable analyses of clinic-pathologic parameters of overall survival in patients with GBM.

Parameter		HR	95% CI	*P*
Gender	categorical	1.27	0.951-1.7	0.105
Age	continuous	1.01	0.994-1.02	0.288
KPS-70	<70 vs 70 and above	0.982	0.682-1.41	0.922
Treatment	None vs TMZ or IR alone	0.117	0.0678-0.201	<0.001
Treatment	None vs TMZ+IR (Stupp protocol)	0.0358	0.0202-0.0632	<0.001
miR-575	High vs low	**1.21**	1.04-1.4	**0.012**
miR-575 is an independent prognostic biomarker correlated with **worse overall survial** in GBM.				

Table 1: Multiple variable analysis of miR-575 expression using the following covariables: gender, age, treatment, and Kornofsky Performance Scale (KPS). miR-575 was found to be significant independent of these variables (p: 0.012; HR: 1.21; 95%CI (1.04-1.4)).

Table 2 Multivariable analyses of clinic-pathologic parameters of overall survival in patients with GBM.

Parameter		HR	95% CI	*P*
Gender	categorical	1.26	0.891-1.79	0.189
Age	continuous	1	0.986-1.02	0.959
KPS-70	<70 vs 70 and above	0.791	0.516-1.21	0.282
Treatment	None vs TMZ or IR alone	0.127	0.0678-0.237	<0.001
Treatment	None vs TMZ+IR (Stupp protocol)	0.042	0.0216-0.0818	<0.001
MGMT methylation	categorical	0.985	0.691-1.41	0.935
miR-575	High vs low	**1.1**	0.912-1.32	**0.323**

Table 2: Multiple variable analysis of miR-575 expression using the following covariables: gender, age, treatement, Kornofsky Performance Scale (KPS), and *MGMT* methylation status. miR-575 was not found to be significant independent of these variables (p: 0.323; HR: 1.1; 95% CI (0.912-1.32).

4.2 Current knowledge of miR-575

While miR-575 was found to be significantly correlated with worse overall survival in GBM based on our study, miR-575 has also been found to be implicated in gastric, lung, breast, and esophageal cancers [19-22]. No publications currently exist regarding miR-575 and gliomas to our knowledge. However, miR-575 has been shown to have both oncogenic and tumor suppressive effects in cancer. High expression of miR-575 is found

in non-small cell lung cancer (NSCLC) tissues, and promotes cell proliferation, migration and invasion of NSCLC cells (26), but in breast cancer, miR-575 reduces cell growth and motility (27). miR-575 signature profiles have also been used to distinguish esophageal adenocarcinoma from Barrett's esophagus, significantly impacting treatment decisions(28). In addition, microarray analyses in lymphoblastoid cell lines suggest than miR-575 may be negatively associated with cell-cycle genes (29). Furthermore, miR-575 is significantly upregulated in human gastric cancer (30).

5. Summary

Based on the preliminary clinical data, we hypothesized that miR-575 plays an oncogenic role in GBM tumorigenesis by inhibiting tumor-suppressor gene function either post-transcriptionally or post-translationally. Additionally, we hypothesize that miR-575 contributes to treatment resistance in GBM.

Herein, we sought to determine the role of miR-575 in proliferation, colony formation, and migration in GBM. In addition, we aimed to elucidate the molecular mechanisms that miR-575 targets. Lastly, we endeavored to determine the role of miR-575 in therapeutic sensitivity in GBM.

Materials and Methods

Cell Culture

The GBM cell lines LN18, LN229, T98G, U251, and U87 were purchased from ATCC. Normal human astrocytes (NHA) were purchased from Lonza. U87/EGFRvIII cells were provided by Deliang Guo (The Ohio State University). All of these cell lines were grown in DMEM media (Gibco) with 10% (v/v) fetal bovine serum (FBS) and 100U/mL penicillin/streptomycin (Sigma). GBM30, a primary patient-derived cell line, was provided by Balveen Kaur (The Ohio State University). GBM30 cells were grown in a neurobasal medium, supplemented with B27 (1×), Heparin (2µg/ml), EGF (20ng/ml), and FGF (20ng/ml). All cells were cultured in a 5% CO_2 sterile environment at 37^{o}C.

Transfection of miRNA mimics, inhibitors and anti-miRNAs

Twenty-four hours prior to transfection, 3 X 10^5 cells were seeded into 60 mm dishes. Cells were counted using a manual cell counter. The total cell number in all four quadrants was averaged and multiplied by 10^4 cells/mL. Media was first aspirated from 60 mm dishes and replaced with DMEM media containing 10% FBS and no antibiotics before transfection. Opti-MEM media (Gibco), Lipofectamine 2000 (Invitrogen), and miR-575 mimic, inhibitor and anti-miR-575 (Ambion) were used for transfection.

Cell Proliferation Assay

Cells (3 X 10^5) were seeded into 60 mm dishes and transfected the following day. Twenty-four hours after transfection, cells were reseeded into a 96-well plate with 1000 cells/100 uL in each well. Five replicates were used for each treatment group at each of five time points. The time points analyzed during this experiment were 24, 48, 72, 96, and 120 hours post-transfection. Each day, cells were washed with 1X PBS and fixed with 4%

paraformaldehyde for 15 minutes. Cells were then stained with methylene blue for twenty minutes and were dried overnight. The following day, 100 uL of solvent (10% acetic acid, 40% H2O, 50% methanol) was applied to each well, and the plate was shaken for twenty minutes. The optical density (OD) value was then measured at an absorbance of 620 nanometers. Experiments were repeated in triplicates.

Colony Formation Assay

Twenty-four hours following transfection, 100-500 cells in 2 mL were seeded into 6-well plates. Three replicates were used per treatment group. Cells were allowed to grow for 10-14 days before harvesting. Cells were then washed with 1X PBS, and 0.5% crystal violet solution (2.5g crystal violet, 375 mL H2O, 125 mL methanol) was applied. Colonies were counted manually using a microscope (31).

Migration Assay

Twenty-four hours following transfection, 700 uL of DMEM media was placed in the lower chamber of each well in a 24-well plate to be used as a chemoattractant. 1 X 10^4 cells in 300 uL of DMEM media were seeded into each the upper chamber of the transwell. Three replicates were used per treatment group. Forty-eight hours later, the upper chamber was scrubbed with a cotton swab to remove non-migratory cells. Cells were then stained with 0.5% crystal violet solution (2.5g crystal violet, 375 mL H2O, 125 mL methanol) for 25 minutes. Cells were rinsed with running water and allowed to dry overnight. Cells were counted the following day using a microscope.

RT-qPCR Analysis of miRNA Expression

Total RNA was isolated from GBM cells using the Trizol reagent (Invitrogen) and measured using a spectrophotometer (ThermoFisher). Total RNA (100 ng) was then

reverse transcribed using the TaqMan MicroRNA Reverse Transcription Kit (Applied Biosystems). The resulting cDNAs were then used in PCR to detect miR-575 expression levels by measuring reporter fluorescence (BioRad). Primers and probes for miR-575 and endogenous controls, RNU48 and RNU6B, were provided by the Taqman Small RNA Assay (Applied Biosystems). Experiments were performed in triplicates and analysis completed using the BioRad CFX Manager software.

RT-qPCR Analysis of mRNA Expression

Total RNA was isolated from GBM cells using Trizol (Invitrogen) and measured using a spectrophotometer (ThermoFisher). Total RNA (1000 ng) was then reverse transcribed using the High Capacity RNA to cDNA kit (Applied Biosystems). cDNA was then amplified by PCR using SYBR Green master mix (Qiagen) and primers for *BLID* (F: 5'-ATGATGTTGTGTTTGGAGAAAAGA-3'; R: 5'-GCTTTGCATAAGCACGGTGTTA-3'), *p27* (F: 5'-TGGAGAAGCACTGCAGAGAC-3'; R: 5'-GCGTGTCCTCAGAGTTAGCC-3'), *KLF6* (F: 5'-ATCAGCCCTCTTTTCCGGTG-3'; R: 5'-TTCTTCTCTTCGGTCCGCTG-3'), *SCAI* (F: 5'-CAGAGGTTCTGGTGATAGCAGT-3'; R: 5'-CCAAGACTTGTCGATGCTGC-3'), *WDFY3* (F: 5'-GGAAATGCTCCGCCGAATACAA-3'; R: 5'-CTCTACTGGCTTCTTCACTCTG-3') and *TSG101* (F: 5'-AGTCTGACTGTGGGTGTTTC-3'; R: 5'-TATGGCTACTGGACACATAC-3') (Invitrogen). *GAPDH* was used as endogenous control (Invitrogen). Experiments were completed in triplicate.

Western Blot

Western blot was performed for BLID and p27 protein, with GAPDH and Lamin-B as endogenous controls. Proteins were isolated using RIPA buffer (Invitrogen) and protease

inhibitors. Protein concentration was measured using the BCA Assay (ThermoFisher) with MikroWin 2000 software. Western blots were run using 4-15% Mini-Protean pre-cast gels (BioRad) at 120 V for one hour in 1 X running buffer (BioRad). Gels were then transferred to nitrocellulose blotting membranes in 1 X transfer buffer (BioRad) for 90 minutes at 0.3 A in the 4^{o}C room. Membranes were then blocked using 5% blocking milk in 1X Tris buffered saline with tween (TBS-T) for one hour. Membranes were then placed in primary antibodies at a 1:1000 concentration overnight in the 4^{o}C room. Primary antibodies were purchased for the proteins BLID (Abcam), p27 (Abcam), Lamin-B (Cell Signaling), and GAPDH (Cell Signaling). Membranes were washed the following day with 1X TBS-T for 15 minutes. Next, membranes were placed in 1:1000 polyclonal anti-mouse or anti-goat secondary antibodies conjugated with horseradish peroxidase for one hour (Abcam). After washing, ECL Plus Western Blotting Detection System (Millipore) was used for detection of horseradish peroxidase activity. Bands were quantified using ImageJ software.

Plasmid Construction

The primers for the *BLID* 3'UTR were first designed using Primer Blast (NCBI) and Ensembl genome browser. The forward primer is 5'-CCGCTCGAGCGGTGAGTTAGGACAGATGCAGCAA-3', and the reverse primer is 5'-ATAAGAATGCGGCTAAACTATTGCAAGATTTGTTTTAATTAAATG-3' (Invitrogen), including sites for the restriction enzymes *XhoI* and *NotI*. PCR was performed using the Platinum Taq Polymerase High Fidelity Kit (ThermoFisher) and genomic DNA previously isolated from U251 cells used as a template. A 1.5% agarose gel (1.5 g agarose, 100 mL 1X TAE Buffer) was made with 5 uL of ethidium bromide. 5 uL of PCR product was used

in gel electrophoresis to confirm the correct product was synthesized. The gel was run again with 45 uL of PCR product. After the second time the gel was run, the DNA band was cut out and gel extraction was performed using the QIAquick Gel Extraction Kit (Qiagen). Next, the *BLID* 3'UTR and pCheck2-reporter luciferase vector were digested at 37 °C using the restriction enzymes *XhoI* and *NotI* overnight. The digested products were then purified using the QIAquick PCR Purification Kit (Qiagen). Then, 25ng vector and 75ng 3'UTR were ligated together using T4 DNA Ligase (Invitrogen). Transformation was then performed using max-efficiency DH5α competent cells protocol (ThermoFisher). Agar plates were made using 15 g of agar in 1 L of LB Broth. Ampicillin was added 1:1000 dilution. 12 mL of the mixture was added to each 10 mL dish (Sigma). Following transformation, agar dishes were incubated in 37^{o}C overnight. Clones were checked the following day and 3'UTR plasmids were then isolated using the QIA Spin Miniprep Kit (Qiagen). Digestion was performed again, and gel electrophoresis was used to confirm both the vector and the plasmid size. Then, 450 ng of DNA was used for Sanger sequencing to ensure the correct product was isolated. Three of the ten isolated clones were confirmed to be the correct *BLID* 3'UTR sequence and were later used for transfection in luciferase assays.

Site-direct mutagenesis

In order to synthesize the *BLID* 3'UTR mutant, the Q5 Site Directed Mutagenesis Kit (BioLabs) was used. The miR-575 binding site on *BLID* was mutated from 5'-AACTGGCT-3' to 5'CAATTGTT-3' in a 4 bp mutation and confirmed with Sanger sequencing. The forward *BLID* 3'UTR 4 bp mutant primer is 5'-TGTTAGTTAAAAGTAAATGGCATTTAATTAAAAC-3', and the reverse primer is 5'-

ATTGTATCCTTTTTAAAAATTTTATTGTTTCTC-3'. The miR-575 binding site on *BLID* was also mutated to 5'-CAATTGCT-3' in a 3 bp mutation and confirmed with Sanger sequencing. The forward *BLID* 3'UTR 3 bp mutant primer is 5'-TGCTAGTTAAAAGTAAATGGCATTTAATTAAAAC-3', and the reverse primer is 5'-ATTGTATCCTTTTTAAAAATTTTATTGTTTCTC-3'.

Dual-Reporter Luciferase Assays

The 3'UTR of *BLID* was constructed, inserted, and annealed to the pCheck2 luciferase vector. The 3'UTR of *p27* was also inserted and annealed to the pCheck2 luciferase vector after purchase (OriGene). For *BLID*, cells were co-transfected with 50 pg of either miR-575 mimic or control and 2 ug of *BLID* wildtype or mutant 3'UTR plasmids. For *p27*, cells were co-transfected with either 50 pg miR-575 mimic or control and 2 ug of *p27* wildtype 3'UTR plasmids. Forty-eight hours later, 5000-10000 cells/100 uL were reseeded into a 96-well plate, with five replicates per treatment group. 24 hours later, the dual-reporter luciferase assay (Promega) was performed, and the results were analyzed using a luminometer.

Temozolomide Sensitivity Assay

Twenty-four hours following transfection, cells were then reseeded into a 96-well plate. The following day each treatment group received temozolomide in concentrations of 0, 10, 20, 50, 100, 250, or 500 uM. Seventy-two hours post-treatment, cells were fixed with 4% paraformaldehyde and stained with methylene blue, according to the previously described protocol for the proliferation assay. Experiments were completed in triplicate.

Radiation Sensitivity Assay

Twenty-four hours following transfection, cells were reseeded into 6-well plates with concentrations of 100, 200, 500, 1000 or 5000 cells in 2 mLs. Twenty-four hours later, each treatment group was irradiated with 0, 2, 4, 6 or 8 Gray (Gy), respectively. Cells were grown for 10-14 days and then stained using crystal violet method previously mentioned for the colony formation assay.

Target Analysis

Target genes were analyzed in silico using miRNA databases TargetScan (http://www.targetscan.org/vert_71), microrna.org (http://www.microrna.org) and miRDB (http://www.mirdb.org/). Databases were analyzed together using GeneVenn (http://genevenn.sourceforge.net/). Common targets among the databases were first analyzed, as well as targets that exhibited strong roles in oncogenesis based on previous publications (PubMed).

Statistical Analysis

For the univariable analysis, Nanostring data was used to determine correlation between Nanostring miRs and overall survival. miR-575 was median dichotomized, and the data were log2 transformed to determine the association between miR-575 dichotomized expression and overall survival (univariable analysis). Other statistical analyses were performed using the software package SPSS 19.0 (SPSS, Chicago, USA). Student's t-test was carried out to detect differential miRNA and mRNA expression. P-values were calculated two-sided, and values less than 0.05 were considered to be statistically significant. Cox3 regression analysis was used for the multivariable analysis. Age, treatment, Kornofsky Performance Scale, and gender were used as covariables.

Results

Overview

Based on univariable and multivariable survival analyses, miR-575 demonstrated a strong negative correlation with overall survival in glioblastoma using a patient cohort from Utrecht (n=268). Following these analyses, a number of experiments were conducted to evaluate the physiological relevance of miR-575 in GBM cell lines. In addition to functional experimentation, a mechanistic study was conducted to determine potential target genes of miR-575. Specifically, *p27/CDKN1B* and *BLID/BRCC2* were investigated in depth due to their promising value *in silico* analyses. Lastly, a therapeutic study was conducted to determine if miR-575 played a role in radiation or temozolomide sensitivity, which are the current standards for GBM patient treatment.

miR-575 *Expression in GBM Cell Lines*

In order to select the most appropriate cell lines for experimentation, qRT-PCR was used to detect endogenous miR-575 expression in one normal human astrocyte (NHA) cell line and seven GBM cell lines (GBM30, LN18, LN229, T98G, U251, U87MG, and U87MG/EGFRvIII). In Figure 6, all seven GBM cell lines trend toward increased miR-575 expression when compared to NHAs. It is important to note that our initial RT-qPCR revealed low endogenous miR-575 expression in LN229 and U251 cells and high endogenous miR-575 expression in U87MG cells. After noticing that there was a discrepancy in the control RNU6B, the experiment was repeated three times using a new control RNU48 to yield the results in Figure 6.

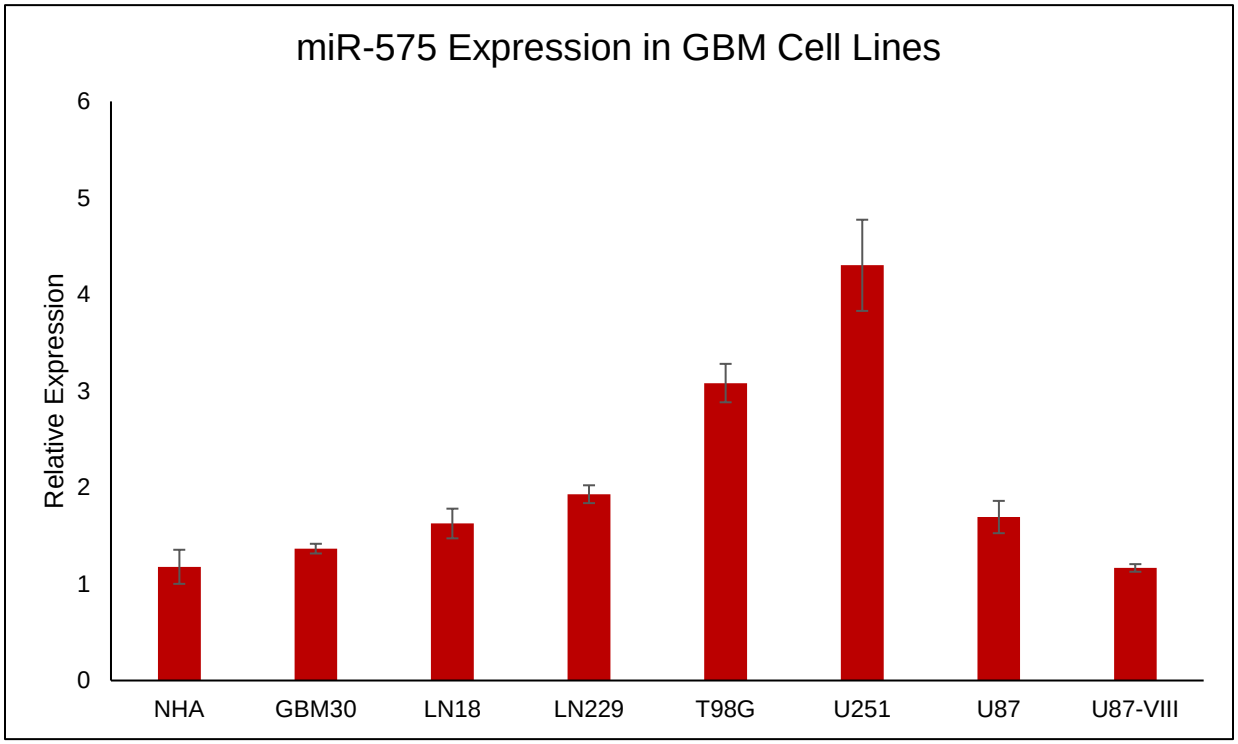

Figure 6: Relative miR-575 expression is shown normalized to normal human astrocytes (NHA). Transcript levels were normalized by RNU48. n=3.

Cell Proliferation

Since proliferation is a hallmark of tumorigenesis in GBM, we sought to determine if miR-575 overexpression contributed to increased growth in GBM cell lines. Proliferation assays were conducted using LN229, U251, and U87MG cells. LN229 and U251 cells were used for miR-575 overexpression due to our initial RT-qPCR results indicating low endogenous miR-575 expression. U87MG cells were used for miR-575 inhibition due to their high endogenous miR-575 expression in the initial RT-qPCR. Figure 7 shows increased proliferation in both LN229 and U251 when transfected with miR-575 mimic (A; B). In addition, Figure 8 shows proliferation decreased in U87MG when treated with anti-miR-575 inhibitor. Both results indicate that higher expression of miR-575 increases cell proliferation.

A.

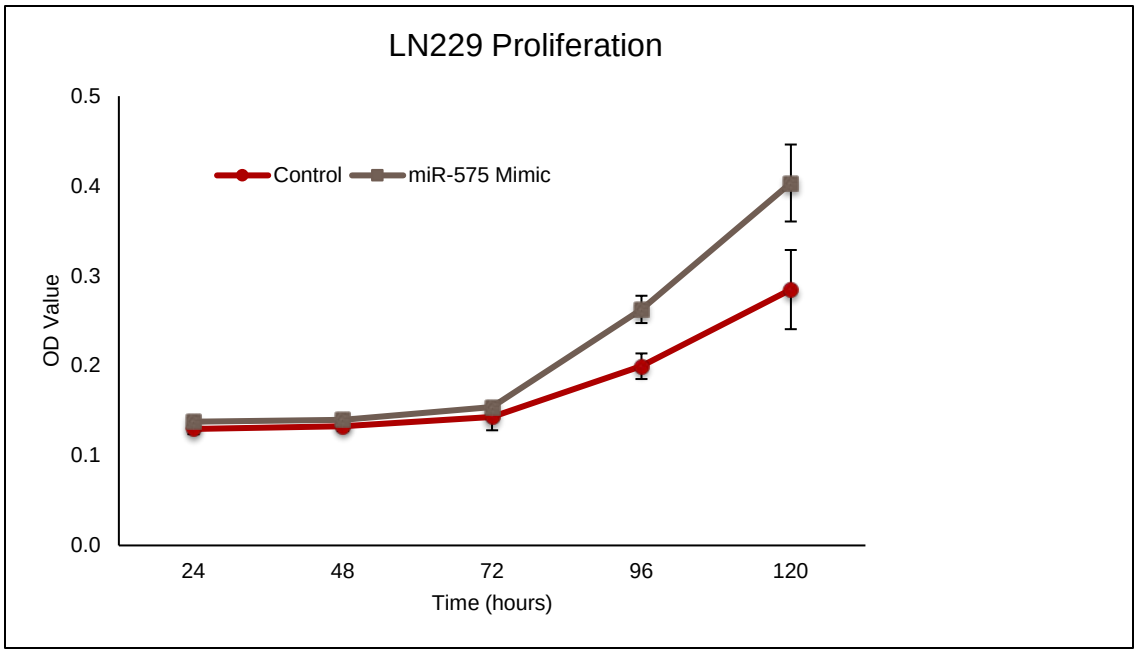

B

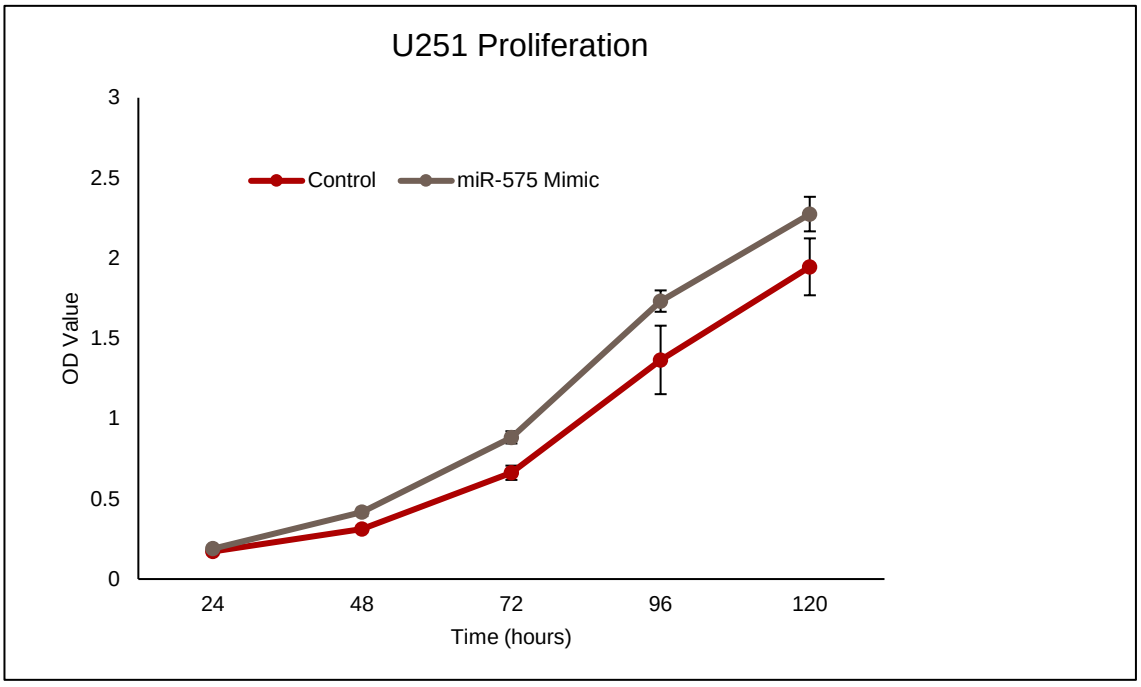

Figure 7: LN229 and U251 cells were transiently transfected with miRNA negative control or miR-575 mimics, respectively. Cell proliferation assays were performed using methylene blue assay at different time points. n=5.

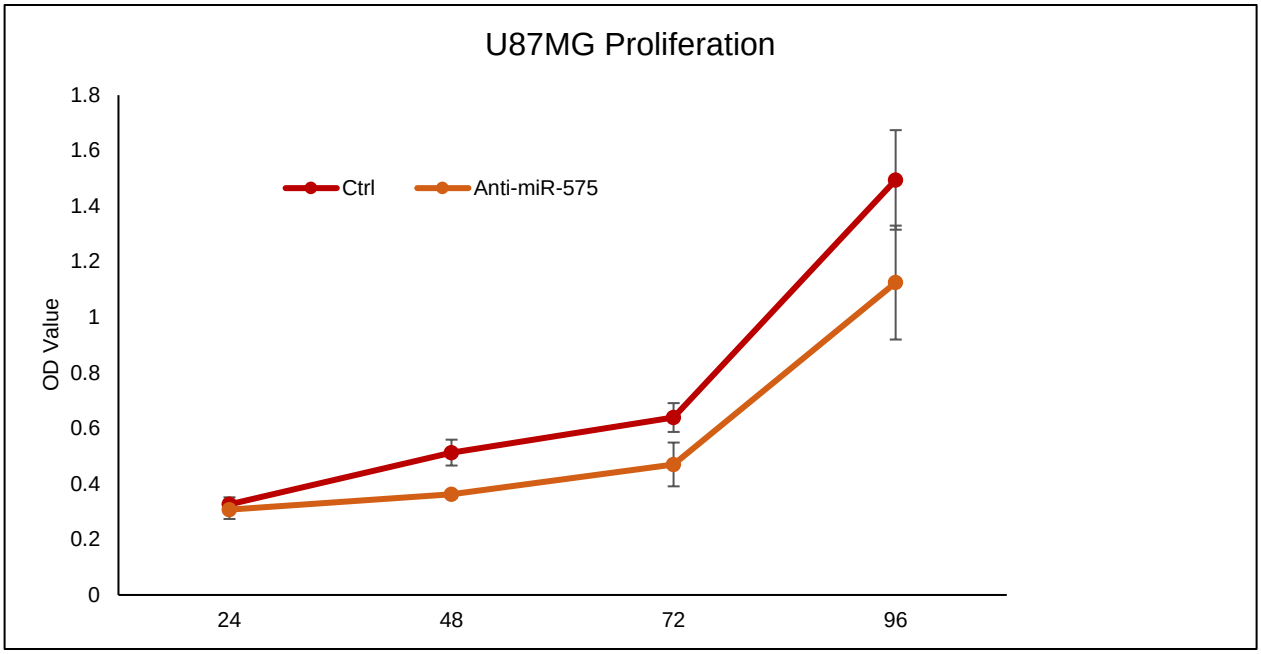

Figure 8: U87MG cells were transiently transfected with miRNA negative control or anti-miR-575 inhibitor. Cell proliferation assays were performed using methylene blue assay at different time points. OD values at 48 and 120 hours are statistically significant using an unpaired t-test (p=0.0117; p=0.0066). n=5.

Colony Formation Assay

Colony formation was assessed in the LN229, U251, and U87MG cell lines to determine if miR-575 expression affects growth of colonies in GBM cells. Colonies were imaged 10-14 days following transfection with miR-575 mimic. Figure 9 shows increased colony formation in LN229 and U251 cells transfected with miR-575 mimic due to low endogenous miR-575 expression; U87MG cells were used for miR-575 inhibition due to high endogenous miR-575 expression. U87MG cells exhibit decreased colony formation when treated with the miR-575 inhibitor (Figure 10). Both results indicate that higher levels of miR-575 expression lead to increased colony formation in GBM cell lines.

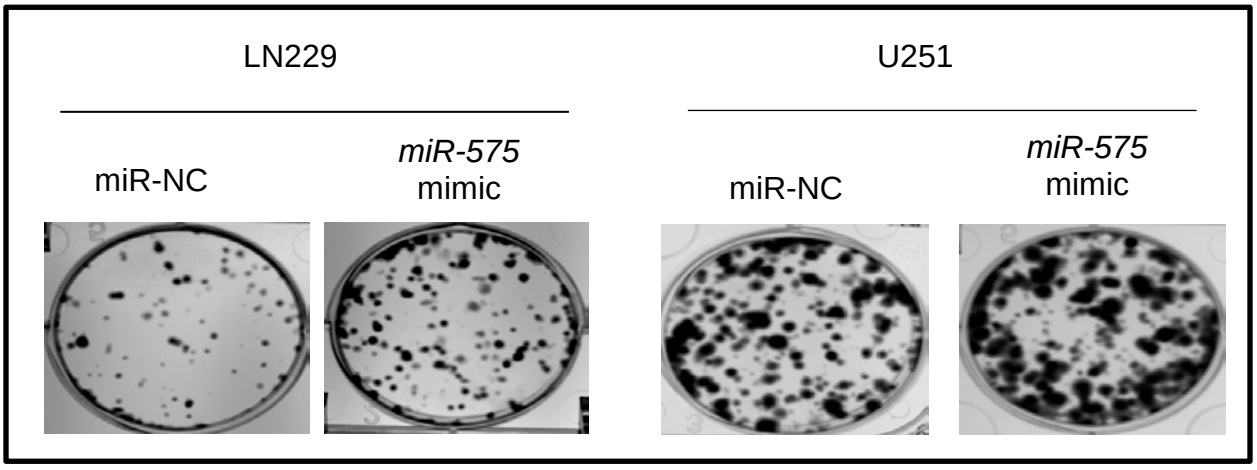

Figure 9: Colony formation assays were performed in LN229 and U251 cells after control or miR-575 mimic transfection. n=3.

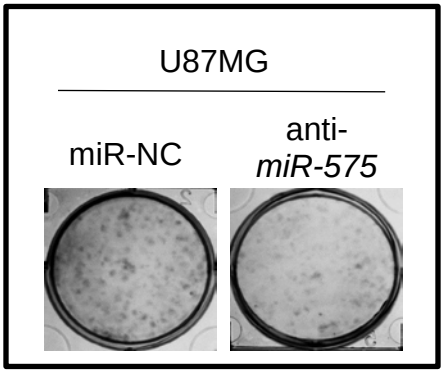

Figure 10: Colony formation assays were performed in U87MG cells after control or anti-miR-575 transfection. n=3

Migration Assay

Migration assays were performed in LN229 and U251 cells to assess the effect of miR-575 on migration in GBM cells. LN229 and U251 cells were used due to their low endogenous miR-575 expression. Migratory cells were stained, imaged, and quantified forty-eight hours after transfection with miR-575 mimic. Figure 11 shows increased migratory cell numbers in cells treated with mimic compared to the control LN229 and

U251 cell lines. Higher miR-575 expression is associated with a greater number of migratory cells.

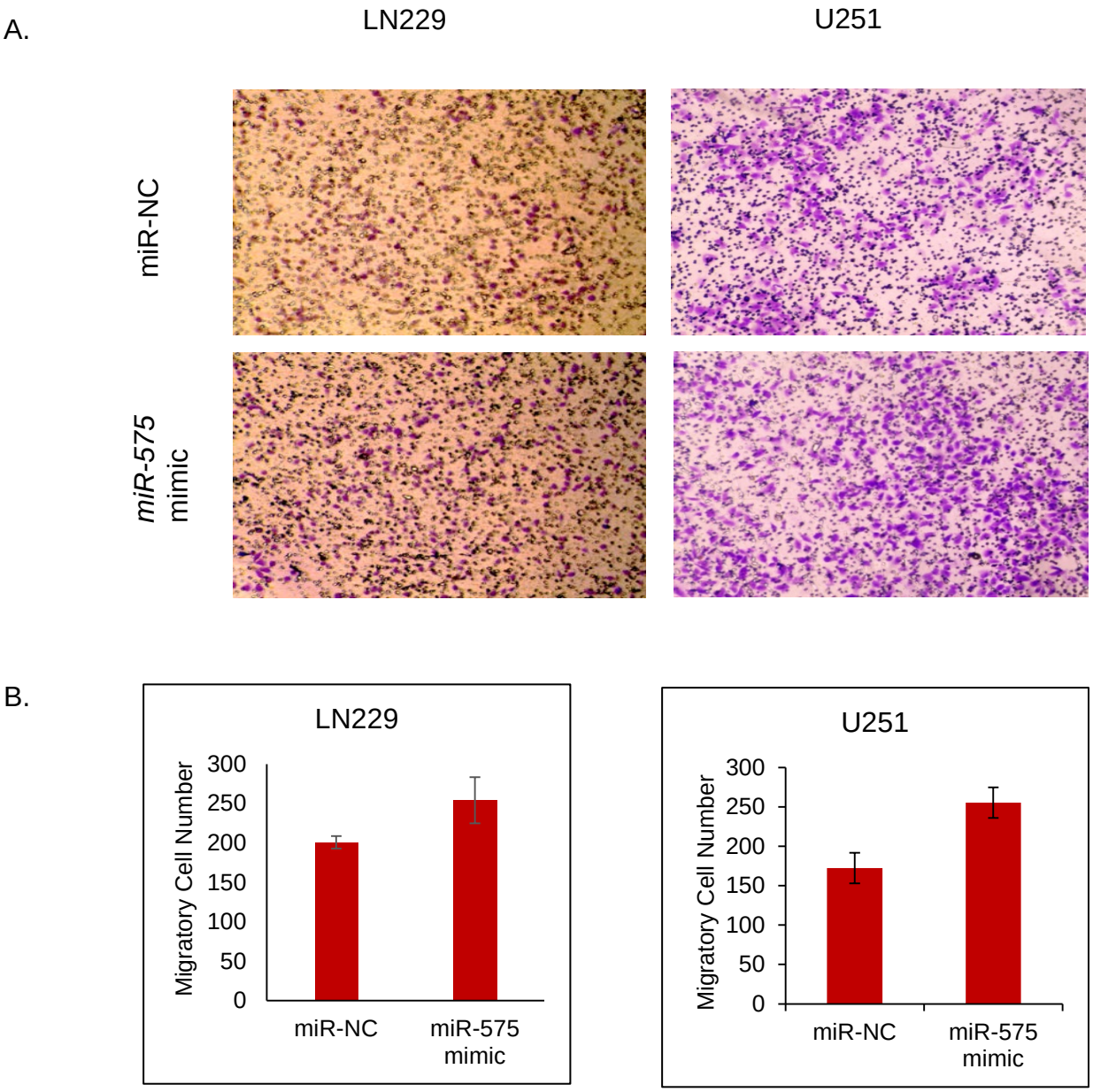

Figure 11: Transwell migration assays were conducted in LN229 and U251 cells after transfection with miR-575 mimic. Numbers of migrated cells were quantified (A; B). Results were not statistically significant using unpaired t-test. n=3.

In Silico Target Gene Analysis

In silico analysis was performed to determine potential target genes of miR-575 using public available databases, miRDB, TargetScan, microrna.org, and miRTarBase. Databases were chosen based upon recommendations in miRNA bioinformatics reviews and previous miRNA publications (32, 33). The databases differ in input, platform, and algorithm used. TargetScan searches for conserved and non-conserved sites within the 3'UTR of protein-coding regions, while taking into account the free energy of the RNA secondary structure (32). MirDB focuses on mature miRNA using a learning algorithm that includes an interactive interface for users. Lastly, microrna.org uses the miRanda algorithm to assess the miR's ability to repress the target gene by utilizing complementarity and free energy analyses (34). miRTarBase manually screens literature and uses a data mining technique to acquire current miRNA findings (35) Six of the same target genes were found in at least three databases using the software GeneVenn (Figure 12). Furthermore, four additional gene targets (*p27/Kip1/CDKN1B, BLID/BRCC2, SCAI, and WDFY3)* were investigated for miR-575 binding sites that were found in at least one microRNA database. These genes were of particular interest due to their function in

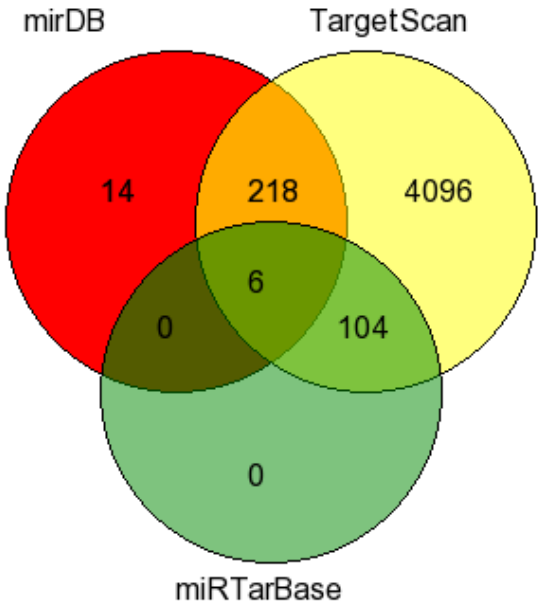

Figure 12: A Venn diagram showing the number of genes that possess a binding site for miR-575 belonging to each database, as well as the combination of databases (GeneVenn).

cancer and previous publications. While the Venn diagram did provide additional targets for investigation, we chose to focus on *BLID* and *p27*, which were only found in two miR databases, because of their roles in carcinogenesis. Notably, it was shown that miR-575 targets the tumor-suppressor *BLID* in NSCLC, promoting tumorigenesis (26). Since the same miRNA may play a role in distinct cancer types, the relationship between miR-575 and *BLID* in GBM was investigated.

Correlation of* miR-575 *and target genes in GBM from the TCGA cohort

Two-tailed Pearson correlation analysis was performed using The Cancer Genome Atlas (TCGA) to assess the correlation between miR-575 and *CDKN1B (p27)/BLID* in a GBM data set (n=159). Data were downloaded from Firebrowse. Figure 13A shows the optimized correlation between miR-575 and *CDKN1B* mRNA expression. Figure 13B shows the optimized correlation between miR-575 and *BLID* mRNA expression. miRNA expression should correlate inversely with target mRNA expression due to the established mechanism of action via mRNA degradation by miRNA. There is a significant negative correlation between miR-575 and *CDKN1B* ($p=5.3 \times 10^{-5}$). However, there does not appear to be a trend between miR-575 expression and *BLID* mRNA expression (p=0.32).

A.

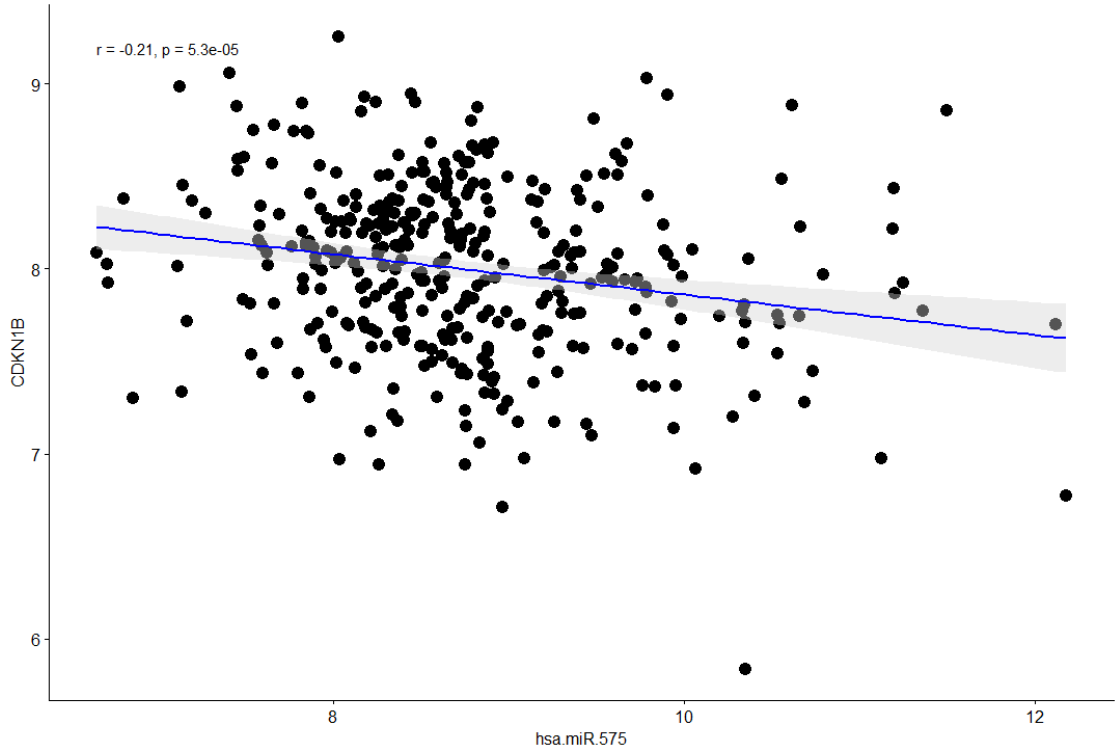

B.

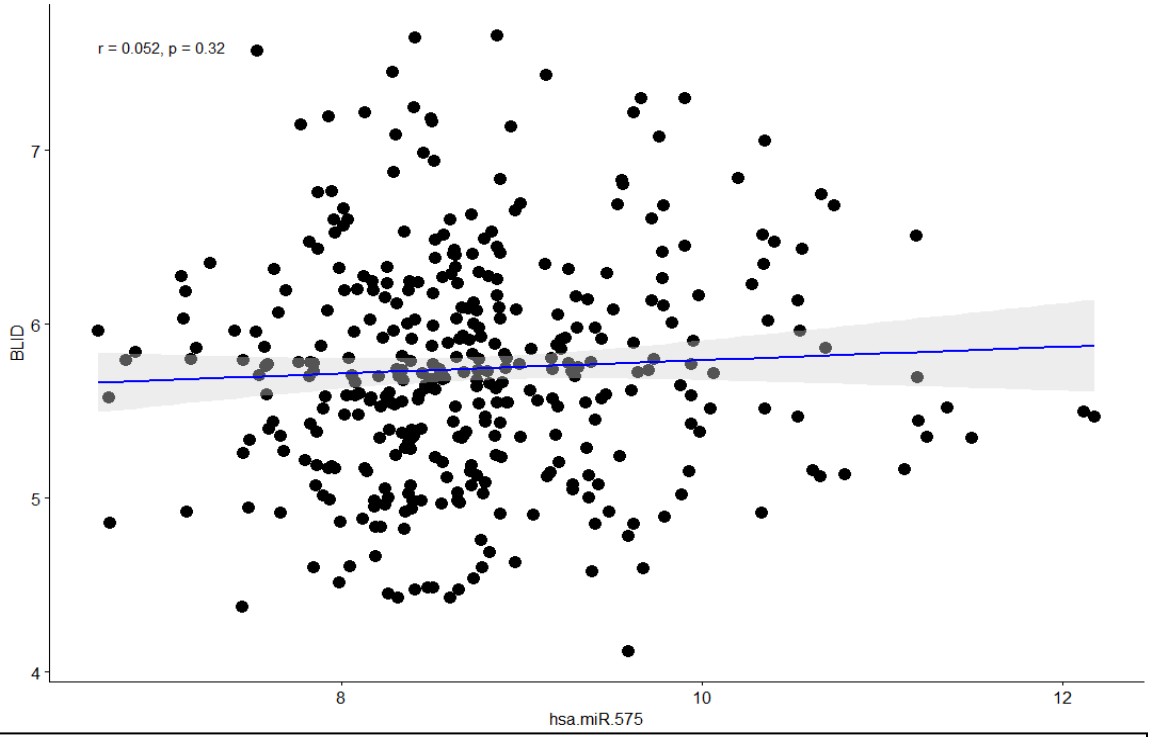

Figure 13: Pearson analysis was performed using the TCGA database. miR-575 expression is compared to *p27/CDKN1B* (A) and *BLID* (B) mRNA expression. CDKN1B possess a statistically significant negative correlation with miR-575 ($p = 5.3 \times 10^{-5}$). The correlation between *BLID* and miR-575 is not significant (p=0.32).

Target Genes of miR-575

p27/CDKN1B

mRNA Expression

RT-qPCR was performed using cDNA from LN229 cells to determine *p27* expression levels after treatment with miR-575 mimic or control. LN229 cells were used for miR-575 overexpression due to their low endogenous miR-575 expression. Figure 14 shows increased *p27* gene expression in cells treated with miR-575 mimic. Higher miR-575 expression is associated with decreased levels of *p27*.

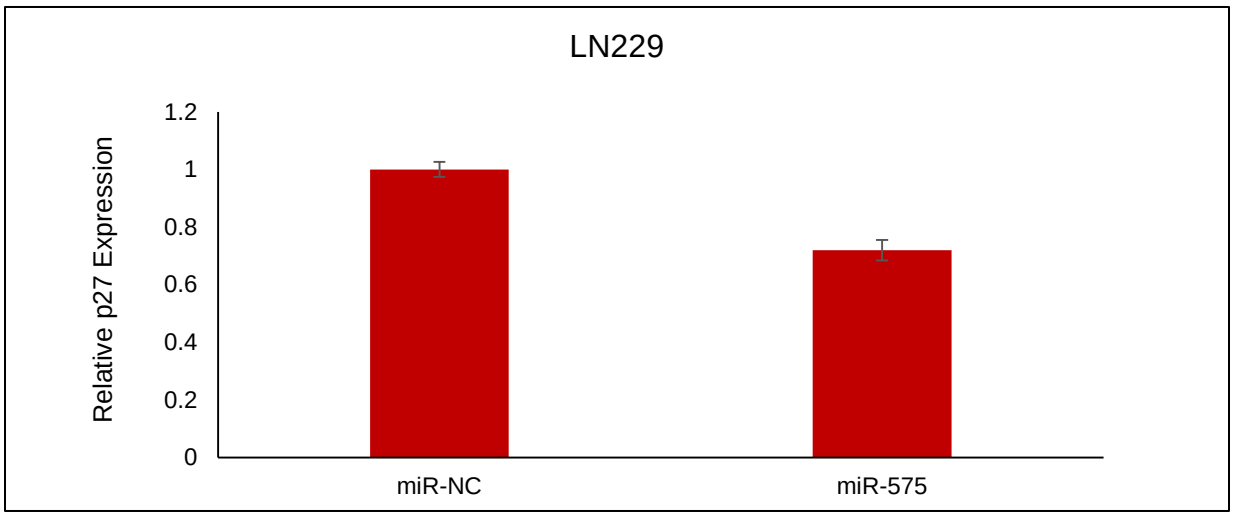

Figure 14: RT-qPCR was performed on cDNA from LN229 cells. *P27* expression levels shown in response to transfection with either mimic or control; results normalized to *GAPDH*. Results were not significant using unpaired t-test.

Western Blot

Western blot was used to detect protein expression of p27 in both LN229 and U251 cells. Overexpression of miR-575 was performed in LN229 and U251 cells due to their low endogenous miR-575 expression. Figure 15 shows p27 protein expression at seventy-two hours post-transfection in LN229 and U251 cells. Both LN229 and U251 cells

exhibited a strong correlation of higher p27 expression in control cells compared to the mimic. Higher expression of miR-575 is associated with lower p27 protein levels.

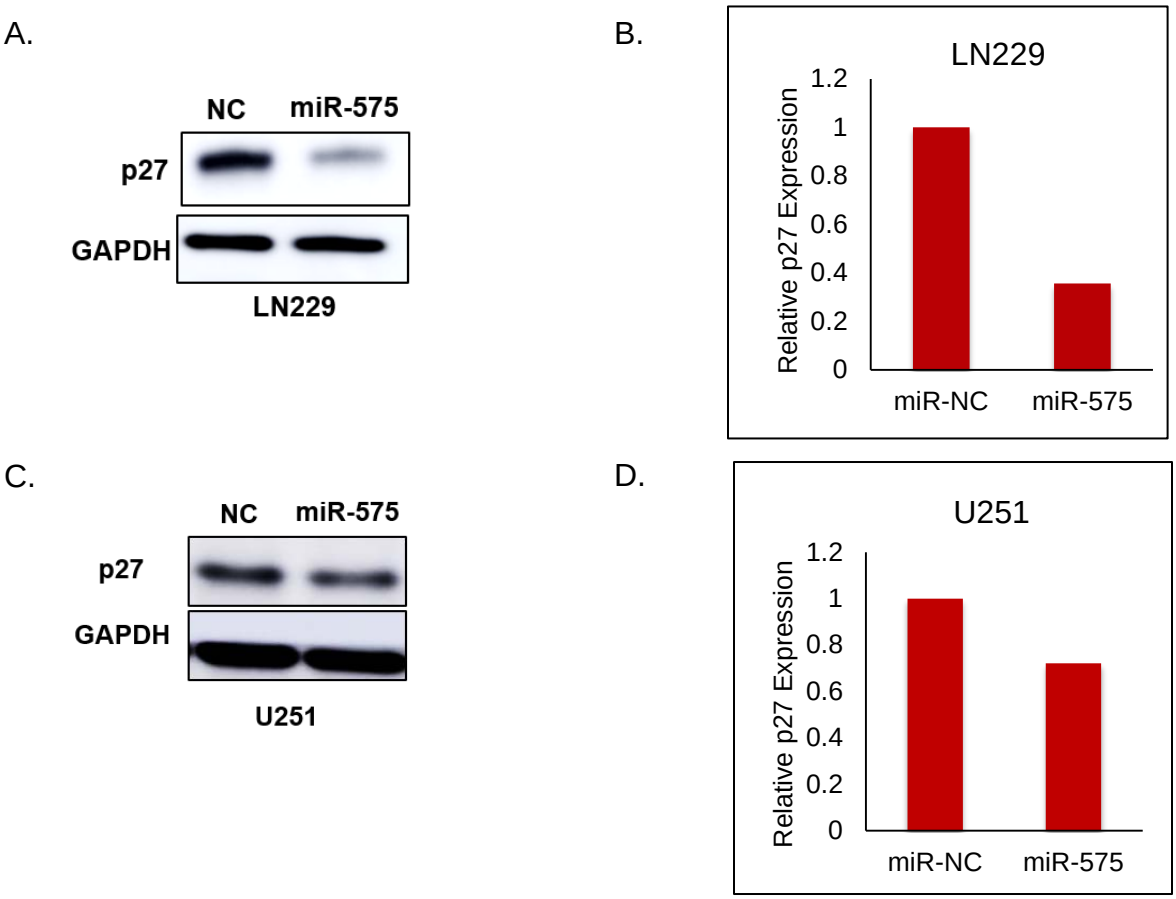

Figure 15: Western blot of p27 protein expression in LN229 and U251 cells 72 hours after transfection (A; C). GAPDH was used as endogenous control. Quantification in LN229 and U251 cells show downregulation of p27 when miR-575 is overexpressed (B; D).

Dual-luciferase reporter assay

Dual-luciferase reporter assays were performed using LN229 and U251 cell lines to determine if there was a direct relationship between miR-575 and *p27* expression. LN229 cells were used for miR-575 overexpression due to their low endogenous miR-575 expression. Figure 16 shows the relative luciferase activity for three treatment groups in both cell lines. *P27* 3'UTR wildtype plasmid, containing *Firefly* and *Renilla*, was

transfected with either control or miR-575 mimic. Both cell lines trend toward reduced luciferase activity when treated with miR-575 mimic at increasing doses.

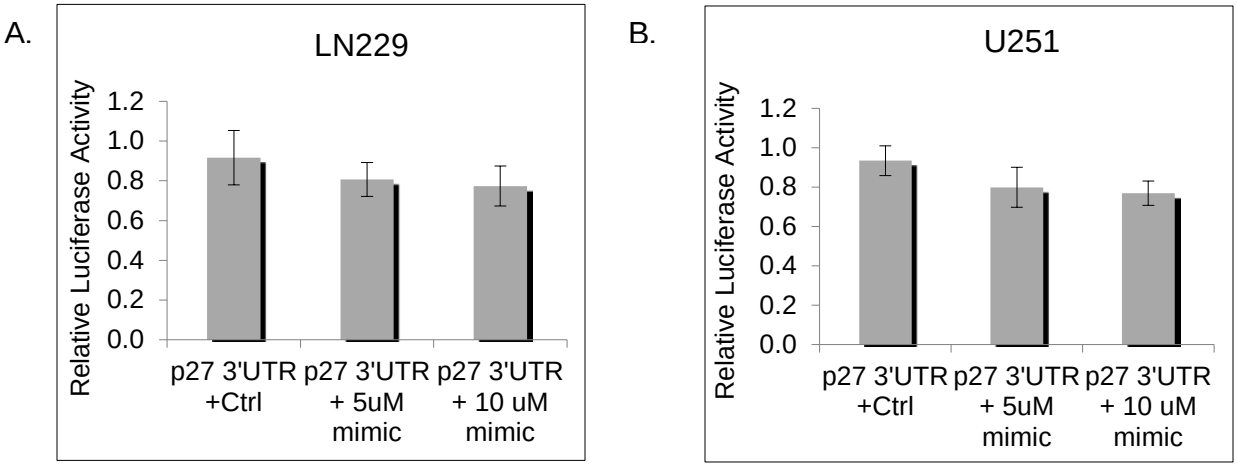

Figure 16: Dual-luciferase reporter assay in LN229 (A) and U251 (B) cells 72 hours post-transfection. Cells co-transfected with p27 3'UTR plasmid and miR-575 mimic exhibit down-regulation in luciferase activity compared to control. Results were not statistically significant using unpaired t-test.

BLID

mRNA Expression

RT-qPCR was performed using cDNA from LN229 and U251 cells to determine *BLID* gene expression levels after transfection with miR-575 mimic, inhibitor, or miRNA negative control. LN229 cells were used for miR-575 overexpression due to their low endogenous levels of miR-575. Detection of *BLID* gene expression in both cells lines showed that cells treated with mimic had decreased *BLID* expression, while cells treated with inhibitor had increased *BLID* expression. Higher expression of miR-575 is correlated with lower *BLID* gene expression (Figure 17).

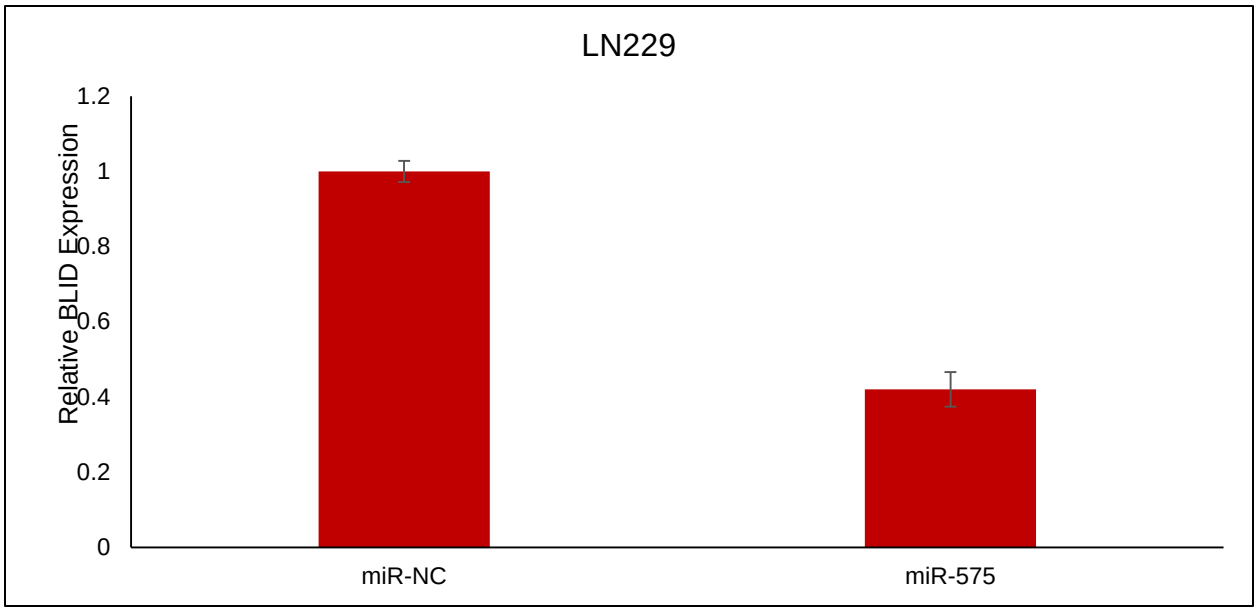

Figure 17: RT-qPCR was performed to measure *BLID* mRNA level in LN229 cells transfected with miRNA negative control or miR-575 mimic. 48 hours post-transfection, cells were harvested for RNA extraction. Results normalized to *GAPDH.*

Western Blot

Western blot was performed using LN229 cells to detect BLID protein expression in cells treated with miR-575 mimic or control. Figure 18 shows imaging and quantification of BLID protein levels seventy-two hours after transfection. LN229 cells exhibit reduced BLID protein expression when miR-575 is overexpressed. Thus, overexpression of miR-575 is associated with lower BLID protein expression.

A.

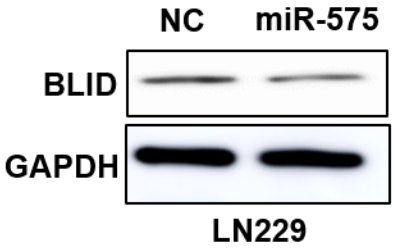

B.

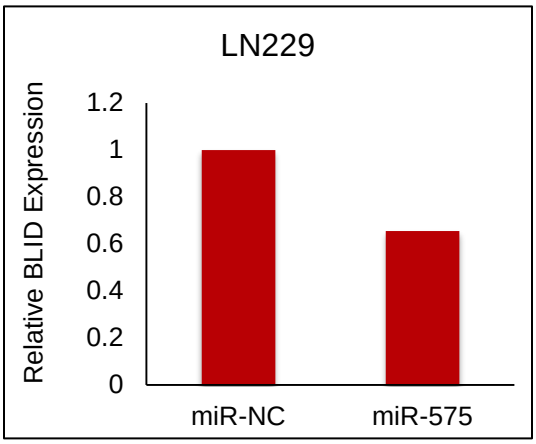

Figure 18: Western blot of BLID protein expression in LN229 cells (A). GAPDH was used as endogenous control. Quantification in LN229 cells show downregulation of BLID protein expression in mimic-treated cells compared to control (B).

Dual-luciferase reporter assay

Dual-luciferase reporter assays were performed using LN229 cells to determine whether a *BLID* and miR-575 have a direct relationship. Figure 19 shows the relative luciferase activity of four distinct treatment groups, each receiving wildtype or mutant *BLID* 3'UTR plasmid co-transfected with either miR-control or miR-575 mimic. Figure 19 shows a reduction in luciferase expression for cells treated with 3'UTR wildtype *BLID* plasmid co-transfected with miR-575 mimic. Reduction is rescued in the miR-575 mimic-treated group when cells are co-transfected with the *BLID* 3'UTR mutant.

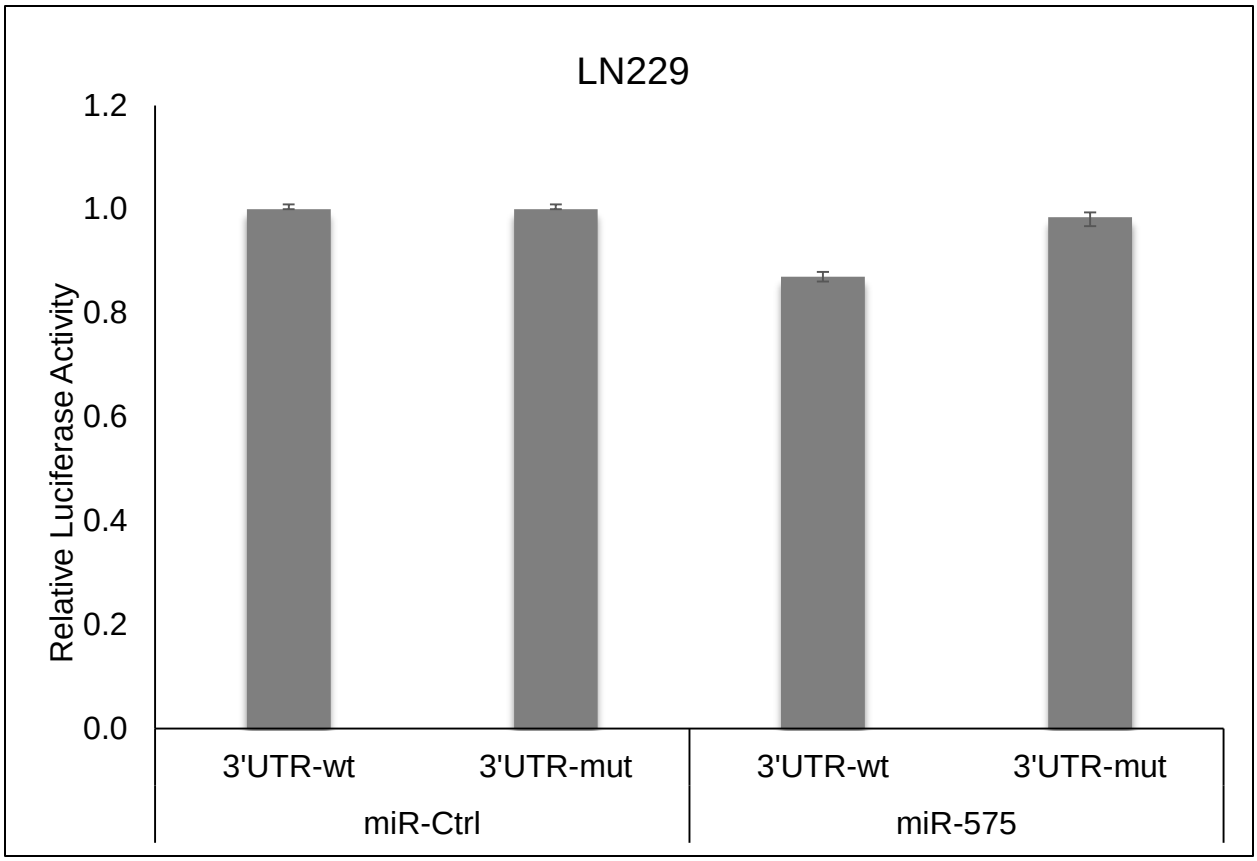

Figure 19: Dual-luciferase reporter assay in LN229 cells. 72 hours post-transfection, relative luciferase activity based on treatment with wildtype or mutant *BLID* 3'UTR plasmid and miR-NC or miR-575 mimic. Cells treated with *BLID* 3'UTR wildtype plasmid exhibit a 20% reduction in luciferase activity compared with all other treatment groups. Results are not statistically significant.

Effect of miR-575 *on temozolomide sensitivity*

Temozolomide sensitivity tests were performed using U87MG/EGFRvIII cells to assess chemotherapy response with varying levels of miR-575 expression. Figure 20 shows the relative proliferation of U87MG/EGFRvIII cells in response to increasing doses of temozolomide. Cells were transfected with miR-575 mimic or control twenty-four hours before treatment. No significant difference was observed between the treatment group and control.

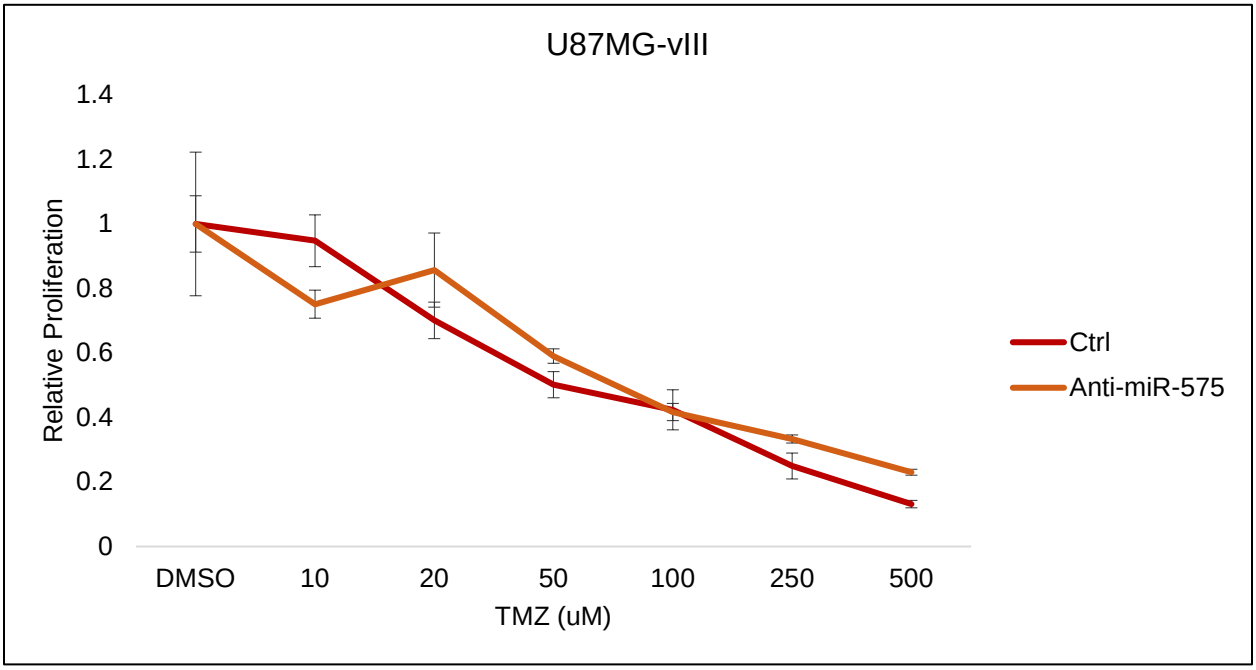

Figure 20: A temozolomide assay was performed for U87MG-vIII cells. Shown is the relative proliferation of cells in response to increasing doses of temozolomide 72 hours following transfection. Results are not statistically significant.

Effect of miR-575 *on radiation sensitivity*

1) miR-575 *expression following radiation*

miR-575 expression following ionizing radiation (IR) was assessed by RT-qPCR using GBM30, T98G, and U251 cells. Figure 21 shows relative miR-575 expression in response to one 8 Gy dose of IR. In Figure 21 both T98G and U251 cells exhibit slightly upregulated miR-575 levels following IR, while GBM30 cells shows a decrease in miR-575 expression levels. The observed trend of miR-575 expression following IR is inconsistent across cell lines which could be due to heterogeneity between cell lines.

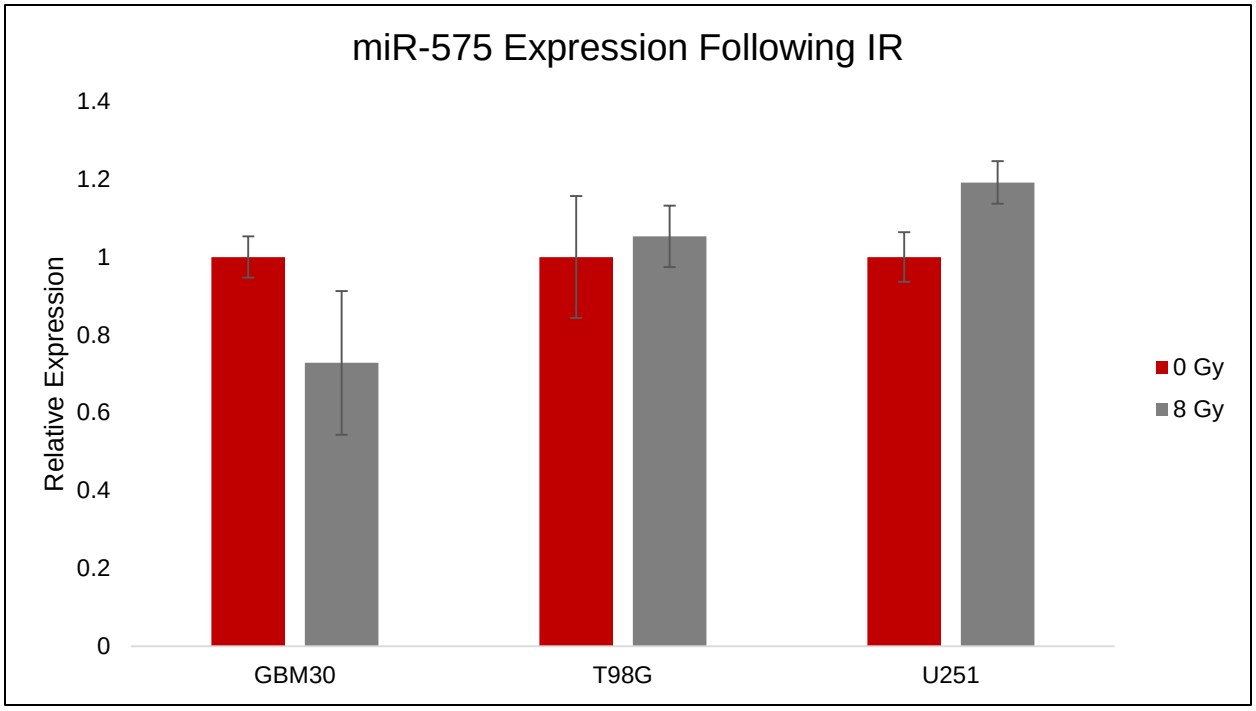

Figure 21: RT-qPCR was performed on cDNA from GBM30, T98G, and U251 cells following radiation with 8 Gy and a control group of 0 Gy. Relative *miR-575* expression levels in response to treatment ten days after IR. Results are not statistically significant.

2) Clonogenic Assay

A clonogenic assay was performed using U251 cells to determine if miR-575 affects the sensitivity of GBM cells to radiation. Figure 22 shows colony formation in control and miR-575 mimic-treated cells at varying IR doses. No significant difference in imaging was observed between the control and miR-575 mimic transfected group. Thus, miR-575 expression does not appear to affect radiation sensitivity. This assay will be repeated in primary glioma cell lines.

A.

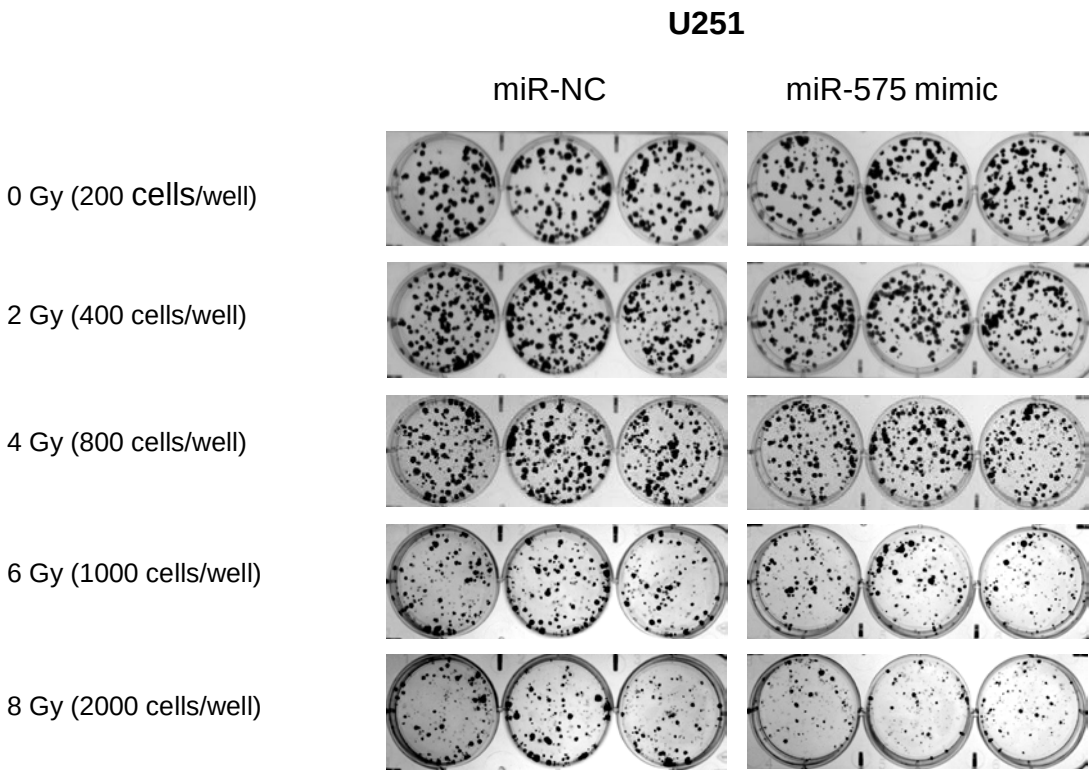

B.

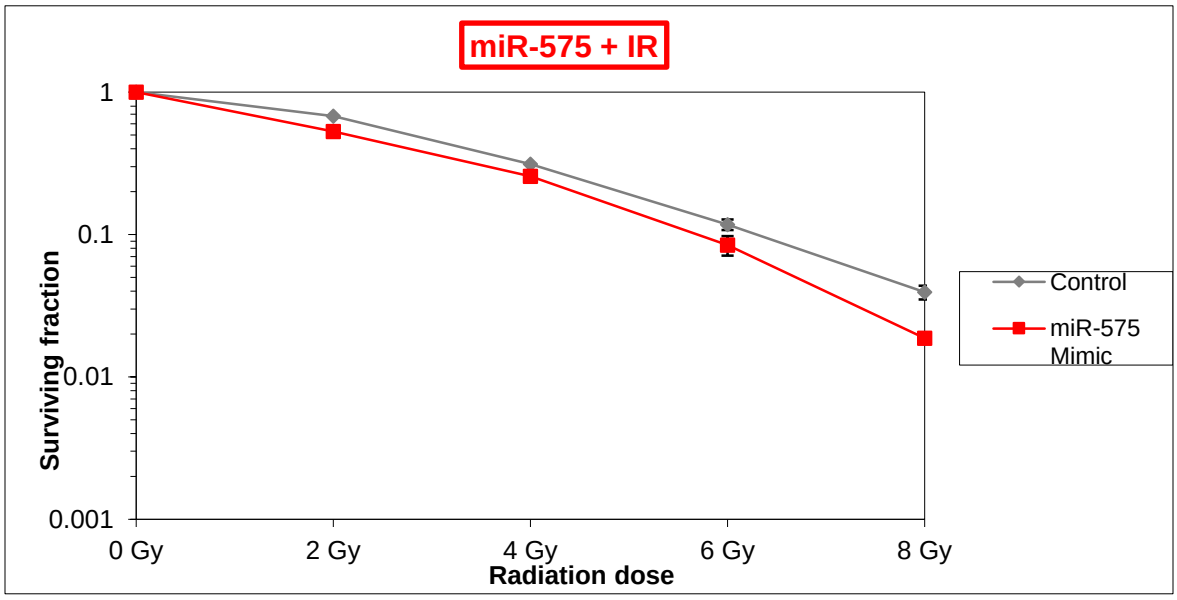

Figure 22: Clonogenic assay in U251 cells. Shown is colony formation following IR in control and miR-575 mimic-transfected cells. Two weeks following radiation, colonies were stained and imaged (A) and surviving fraction was quantified (B). Results were not statistically significant.

Discussion

Key Findings

Currently, new strategies to improve survival outcomes are desperately needed for GBM patients as median survival times remain poor (3). The Stupp protocol, which was implemented in 2005, still remains the standard of care after surgery for most patients (36). Due to the heterogeneity presented in GBM tumors, more personalized medical approaches are necessary to improve overall survival. Epigenetic biomarkers, like miRNAs, are emerging as promising candidates to better characterize GBM patients into more refined prognostic groups (3). miRNAs have been shown to contribute to GBM tumor development and progression, and further insight to these biological mechanisms will likely help to identify novel targets for therapeutic intervention (8). To our knowledge, this study is the first to 1) identify miR-575 as a prognostic biomarker in GBM and to 2) show that miR-575 acts as an oncogene that directly targets the tumor-suppressor genes, *p27* and *BLID*, in GBM. While the oncogenic effect of miR-575 has not been reported in GBM prior to this study, miR-575 has been shown to have both oncogenic and tumor suppressive effects in multiple other cancers. As previously discussed, high expression of miR-575 has been shown to promote cell proliferation, migration and invasion of NSCLC cells (26), but in breast cancer, miR-575 reduced cell growth and motility (27). Additionally, miR-575 signature profiles have been used to distinguish esophageal adenocarcinoma from Barrett's esophagus, significantly impacting treatment modality chosen (28). While the function of miR-575 may vary across cancer types, its significance in tumorigenesis has been validated in multiple cancers, including gastric, lung, breast, and esophageal (26-28).

To further validate that increased miR-575 is associated with worse survival, we evaluated the physiological role of miR-575 in GBM in cell proliferation, colony formation, and migration. We utilized a synthetic miRNA mimic to overexpress miR-575 and a specific antisense oligonucleotide to inhibit miR-575 expression in GBM cells. Overexpression of miR-575 *in vitro* led to increased proliferation, colony formation, and migration, which are all hallmark mechanisms of tumorigenesis in GBM. These findings support the proposed oncogenic role of miR-575 in GBM.

To investigate the underlying molecular mechanisms by which miR-575 promotes tumorigenesis, we identified potential target genes using *in silico* analyses of three miRNA databases in conjunction with current literature. *p27* and *BLID* were identified as the most promising targets due to their frequency among miRNA databases and known roles in carcinogenesis. In order to further validate these targets *in vitro*, qPCR, western blotting, and luciferase assays were performed. Overexpression of miR-575 correlated with down-regulation of p27 and BLID mRNA and protein levels. These results support our hypothesis by exhibiting downregulation of tumor-suppressor genes and protein expression in response to miR-575 overexpression. The correlation observed between miRNA and their target genes is a result of miRNA binding and degrading target gene mRNA or blocking translation. Through luciferase assays, we were able to support the idea that miR-575 binds directly to the 3'UTR of *p27* and *BLID* mRNA to inhibit expression. *p27* and *BLID* may be part of the same pathway or part of a global effect of this miR-575 on GBM cells.

While the relevance of *p27* as a tumor-suppressor gene has been published in glioma, its relationship with miR-575 has not been documented to our knowledge (37-42).

One study reports the anti-proliferative effects of *p27* in glioma cells through activation by *CPEB1* (cytoplasmic element binding protein 1). *CPEB1* is downregulated in GBM and participates in cell cycle by controlling mRNA translation efficiency via the 3'UTR (39). Additionally, increased *p27* expression is shown to improve survival in glioma stem cells *in vivo* via the *FOXOA3/Akt* pathway. Dephosphorylation of *FOXOA3* and *Akt* lead to increased *p27* expression as a result of *CLK2* (Cdc-like kinase 2) depletion (38). Both studies support the tumor-suppressive function of *p27* in GBM. Additionally, one study showed that application of *p27* gene therapy could have a significant impact on malignant glioma treatment. In this study, a *p27* adenovirus inhibited tumor progression *in vitro* (37). *p27* plays a significant role in cell cycle and tumorigenesis, and it is crucial to identify more miRNAs that target it to widen alternative treatment options.

Additionally, the miR-575/*BLID* axis was reported in NSCLC, but has yet to be validated in GBM prior to our study (26). miR-575 also decreased proliferation, colony formation, and migration in NSCLC cells as in our study. A recent study showed that BLID (BRCC2) inhibited metastasis in breast cancer by down-regulating the Akt pathway (43).

To explore the potential role of miR-575 in therapeutic sensitivity, clonogenic and cell viability assays were performed which revealed no effect of miR-575 on radiosensitivity or chemosensitivity, respectively. Based on our findings, miR-575 appears to serve as a prognostic biomarker in GBM, but its effects are independent of treatment and therefore do not promote resistance or sensitivity.

Limitations

This study utilizes GBM the cell lines LN229, U251, and U87, which are cultured cells. Recently, it has been discovered that primary cell lines, undifferentiated and stem-

like, better retain their original genotype and more accurately represent the human GBM phenotype (44). Thus, our study supports miR-575 as a prognostic biomarker in GBM, but in order to confirm our findings, *in vitro* experimentation using primary glioma stem-like cells and *in vivo* studies should be conducted.

Additionally, as in other miRNA therapeutic studies, challenges regarding the ability of miRNAs to cross the blood-brain barrier and target a specific cell type remain. While miR-575 may be used individually as a prognostic biomarker after further validation, other studies have indicated that there are limitations in using a single miRNA to determine prognosis. MiRNA expression levels can change as a result of treatment and some miRNAs are implicated in multiple cancers. These studies suggest using miRNA panels, composed of many miRNAs, to obtain better sensitivity and specificity (8). miR-575 may be used to develop a prognostic miRNA signature in future studies.

While miRNAs have been identified as promising biomarker candidates, their role as potential therapeutic targets warrants careful examination of off-target effects that may lead to adverse side effects. For example, differences in PCR annealing temperatures and physiological temperatures may cause anti-miRs to anneal imperfectly to unwanted target gene areas and cause adverse side effects. Due to the potential for off-target effects in miRNA therapy, individual gene targets such as *p27* or *BLID* may serve as better therapeutic interventions. Despite therapeutic challenges, miRNAs are excellent resources to detect the activity of pathways implicated in GBM tumor progression.

While our physiological data is compelling, the mechanistic data requires further experimentation to confirm *p27* and *BLID* as targets of miR-575. We have not yet mutated the *p27* plasmid to confirm the reduction we observed using the *p27* wildtype plasmid.

Furthermore, the reduction in luciferase activity for both target genes was modest, so we plan to replicate this experiment in additional cell lines to confirm the direct relationship between miR-575 and its target genes.

Lastly, regarding our clinical data, tissues were only obtained from one cohort, so further validation in an independent cohort would strengthen our study's clinical relevance and is warranted to ascertain the future role of miR-575 as a prognostic biomarker.

Future Directions

While our study provides *in vitro* evidence for miR-575 as an oncogene in GBM, experiments should be replicated in primary glioma cell lines, which more closely adhere to human phenotypes, before proceeding with *in vivo* experimentation. Additionally, we plan to further validate the putative targets *p27* and *BLID* due to the discrepancies we observed in mRNA and protein expression. We plan to also pursue an *in vivo* study to further validate the oncogenic role of miR-575 and support our findings of its potential as a biomarker in GBM.

Additionally, we identified other potential target genes *in silico*, but we have not yet attempted to validate these genes *in vitro*. These genes, including *KLF6, SCAI, WDFY3*, and *TSG101*, are all tumor-suppressor genes and are promising candidates to explore due to their roles in tumorigenesis. Of these, *KLF6* and *SCAI* have been previously published in glioma (45, 46).

Regarding the therapeutic role of miR-575, our results indicate that miR-575 has no effect on radiosensitivity and chemosensitivity, but further experimentation is required to confirm this finding. For chemosensitivity, cell viability assays after temozolomide treatment would need to be replicated in additional cell lines. Additionally, this result would

need to be confirmed by using an apoptosis assay with an accompanying western blot assaying apoptosis proteins, cleaved caspase-3 and cleaved caspase-9. For the clonogenics assay experiments such as comet assay or γ-H2AX foci assay should be conducted using additional cell lines to confirm our findings.

In conclusion, our study is the first to identify miR-575 as a biomarker in GBM which is significantly correlated with worse overall survival in a clinical cohort. We propose that miR-575 promotes tumor progression, in part, via direct-targeting of *p27* and *BLID*. Our data suggest miR-575 may be used alone or with other molecular/clinical factors to better characterize GBMs thereby contributing to a personalized medicine approach. Additionally, our study provided insight into the mechanisms of tumor progression in GBM and identified additional promising targets for future therapies.

Conclusion

Based on clinical data suggesting a negative correlation between miR-575 expression and overall survival in GBM, this study was conducted to validate the oncogenic role of miR-575 in GBM. Using *in vitro* experimentation, we were able to show that overexpression of miR-575 increased proliferation, colony formation, and migration in GBM cell lines. Additionally, we identified two promising targets, *p27* and *BLID*, that could serve as alternative points of therapeutic intervention in this tumor progression pathway. However, we did not find that miR-575 plays a role in radiation or chemotherapy sensitivity. Further analyses are needed to confirm these putative targets of miR-575 and to confirm that miR-575 does not affect therapeutic resistance in GBM. We postulate that miR-575 is a likely biomarker in GBM that acts in part by downregulating *p27* and *BLID.* Importantly, this investigation of miR-575 provides further insight into tumor progression in GBM, which can be utilized to identify new targets for future treatments.

Acknowledgements

This work was funded in part by the Summer Undergraduate Research Institute at The Ohio State University with additional funds provided by the National Cancer Institute [R01CA169368 (to A.C), R01CA11522358 (to A.C), R01CA1145128 (to A.C), R01CA108633 (to A.C), and 1RC2CA148190 (to A.C), U10CA180850-01 (to A.C.)]; A Brain Tumor Funders Collaborative Grant (to A.C.); Ohio State University Comprehensive Cancer Center Award (to A.C.). I would like to extend a special thank you to Tiantian Cui, MD, Erica Bell, PhD, Jahar Haque, PhD, Jessica Fleming, PhD, and Arnab Chakravarti, MD for their guidance and support throughout the course of this project. Additionally, I would like to thank my thesis committee members, Gregory Booton, PhD, Christin Burd, PhD, and Christopher Callam, PhD for their time and participation in my thesis defense.

References

1. Ostrom QT, Gittleman H, Stetson L, Virk SM, Barnholtz-Sloan JS. Epidemiology of gliomas. Cancer treatment and research. 2015;163:1-14.
2. Brown DM, Croce C, Nana-Sinkam SP. Chapter 2 - Clinical and Therapeutic Applications of MicroRNA in Cancer A2 - Laurence, Jeffrey. Translating MicroRNAs to the Clinic. Boston: Academic Press; 2017. p. 17-37.
3. Chakravarti A, Palanichamy K, Bell EH. Biomarkers usher in era of personalized care for malignant glioma patients. CNS oncology. 2012;1:3-6.
4. Bell EH, Pugh SL, McElroy JP, Gilbert MR, Mehta M, Klimowicz AC, et al. Molecular-Based Recursive Partitioning Analysis Model for Glioblastoma in the Temozolomide Era: A Correlative Analysis Based on NRG Oncology RTOG 0525. JAMA oncology. 2017;3:784-92.
5. Thakkar JP, Dolecek TA, Horbinski C, Ostrom QT, Lightner DD, Barnholtz-Sloan JS, et al. Epidemiologic and molecular prognostic review of glioblastoma. Cancer epidemiology, biomarkers & prevention : a publication of the American Association for Cancer Research, cosponsored by the American Society of Preventive Oncology. 2014;23:1985-96.
6. Martinez-Garcia M, Alvarez-Linera J, Carrato C, Ley L, Luque R, Maldonado X, et al. SEOM clinical guidelines for diagnosis and treatment of glioblastoma (2017). Clinical & translational oncology : official publication of the Federation of Spanish Oncology Societies and of the National Cancer Institute of Mexico. 2018;20:22-8.
7. Beyer S, Fleming J, Meng W, Singh R, Haque SJ, Chakravarti A. The Role of miRNAs in Angiogenesis, Invasion and Metabolism and Their Therapeutic Implications in Gliomas. Cancers. 2017;9.
8. Huang SW, Ali ND, Zhong L, Shi J. MicroRNAs as biomarkers for human glioblastoma: progress and potential. Acta pharmacologica Sinica. 2018.
9. Ohgaki H, Kleihues P. The definition of primary and secondary glioblastoma. Clinical cancer research : an official journal of the American Association for Cancer Research. 2013;19:764-72.
10. DeWitt JC, Mock A, Louis DN. The 2016 WHO classification of central nervous system tumors: what neurologists need to know. Current opinion in neurology. 2017;30:643-9.
11. Gilbertson RJ. High-grade glioma: can we teach an old dogma new tricks? Cancer cell. 2006;9:147-8.
12. Kim TM, Huang W, Park R, Park PJ, Johnson MD. A developmental taxonomy of glioblastoma defined and maintained by MicroRNAs. Cancer research. 2011;71:3387-99.
13. Losman JA, Kaelin WG, Jr. What a difference a hydroxyl makes: mutant IDH, (R)-2-hydroxyglutarate, and cancer. Genes & development. 2013;27:836-52.
14. Hegi ME, Diserens AC, Gorlia T, Hamou MF, de Tribolet N, Weller M, et al. MGMT gene silencing and benefit from temozolomide in glioblastoma. The New England journal of medicine. 2005;352:997-1003.
15. Bartel DP. MicroRNAs: genomics, biogenesis, mechanism, and function. Cell. 2004;116:281-97.
16. Hayes J, Peruzzi PP, Lawler S. MicroRNAs in cancer: biomarkers, functions and therapy. Trends in molecular medicine. 2014;20:460-9.

17. Peng Y, Croce CM. The role of MicroRNAs in human cancer. Signal transduction and targeted therapy. 2016;1:15004.
18. Janssen HL, Reesink HW, Lawitz EJ, Zeuzem S, Rodriguez-Torres M, Patel K, et al. Treatment of HCV infection by targeting microRNA. The New England journal of medicine. 2013;368:1685-94.
19. MesomiR 1: A Phase I Study of TargomiRs as 2nd or 3rd Line Treatment for Patients With Recurrent MPM and NSCLC.
20. A Multicenter Phase I Study of MRX34, MicroRNA miR-RX34 Liposomal Injection.
21. Xue W, Dahlman JE, Tammela T, Khan OF, Sood S, Dave A, et al. Small RNA combination therapy for lung cancer. Proceedings of the National Academy of Sciences of the United States of America. 2014;111:E3553-61.
22. Onishi M, Ichikawa T, Kurozumi K, Date I. Angiogenesis and invasion in glioma. Brain tumor pathology. 2011;28:13-24.
23. Moller HG, Rasmussen AP, Andersen HH, Johnsen KB, Henriksen M, Duroux M. A systematic review of microRNA in glioblastoma multiforme: micro-modulators in the mesenchymal mode of migration and invasion. Molecular neurobiology. 2013;47:131-44.
24. Zhai GG, Malhotra R, Delaney M, Latham D, Nestler U, Zhang M, et al. Radiation enhances the invasive potential of primary glioblastoma cells via activation of the Rho signaling pathway. Journal of neuro-oncology. 2006;76:227-37.
25. Giese A, Westphal M. Glioma invasion in the central nervous system. Neurosurgery. 1996;39:235-50; discussion 50-2.
26. Wang H, Yan C, Shi X, Zheng J, Deng L, Yang L, et al. MicroRNA-575 targets BLID to promote growth and invasion of non-small cell lung cancer cells. FEBS letters. 2015;589:805-11.
27. Fisher JN, Terao M, Fratelli M, Kurosaki M, Paroni G, Zanetti A, et al. MicroRNA networks regulated by all-trans retinoic acid and Lapatinib control the growth, survival and motility of breast cancer cells. Oncotarget. 2015;6:13176-200.
28. Drahos J, Schwameis K, Orzolek LD, Hao H, Birner P, Taylor PR, et al. MicroRNA Profiles of Barrett's Esophagus and Esophageal Adenocarcinoma: Differences in Glandular Non-native Epithelium. Cancer epidemiology, biomarkers & prevention : a publication of the American Association for Cancer Research, cosponsored by the American Society of Preventive Oncology. 2016;25:429-37.
29. Lee JE, Hong EJ, Nam HY, Hwang M, Kim JH, Han BG, et al. Molecular signatures in response to Isoliquiritigenin in lymphoblastoid cell lines. Biochemical and biophysical research communications. 2012;427:392-7.
30. Yao Y, Suo AL, Li ZF, Liu LY, Tian T, Ni L, et al. MicroRNA profiling of human gastric cancer. Molecular medicine reports. 2009;2:963-70.
31. Franken NA, Rodermond HM, Stap J, Haveman J, van Bree C. Clonogenic assay of cells in vitro. Nature protocols. 2006;1:2315-9.
32. Akhtar MM, Micolucci L, Islam MS, Olivieri F, Procopio AD. Bioinformatic tools for microRNA dissection. Nucleic Acids Res. 2016;44:24-44.
33. Riffo-Campos AL, Riquelme I, Brebi-Mieville P. Tools for Sequence-Based miRNA Target Prediction: What to Choose? International journal of molecular sciences. 2016;17.
34. Betel D, Koppal A, Agius P, Sander C, Leslie C. Comprehensive modeling of microRNA targets predicts functional non-conserved and non-canonical sites. Genome biology. 2010;11:R90.

35. Hsu SD, Tseng YT, Shrestha S, Lin YL, Khaleel A, Chou CH, et al. miRTarBase update 2014: an information resource for experimentally validated miRNA-target interactions. Nucleic Acids Res. 2014;42:D78-D85.
36. Stupp R, Mason WP, van den Bent MJ, Weller M, Fisher B, Taphoorn MJ, et al. Radiotherapy plus concomitant and adjuvant temozolomide for glioblastoma. The New England journal of medicine. 2005;352:987-96.
37. Park KH, Lee J, Yoo CG, Kim YW, Han SK, Shim YS, et al. Application of p27 gene therapy for human malignant glioma potentiated by using mutant p27. Journal of neurosurgery. 2004;101:505-10.
38. Park SY, Piao Y, Thomas C, Fuller GN, de Groot JF. Cdc2-like kinase 2 is a key regulator of the cell cycle via FOXO3a/p27 in glioblastoma. Oncotarget. 2016;7:26793-805.
39. Galardi S, Petretich M, Pinna G, D'Amico S, Loreni F, Michienzi A, et al. CPEB1 restrains proliferation of Glioblastoma cells through the regulation of p27(Kip1) mRNA translation. Scientific reports. 2016;6:25219.
40. Liu X, Liu N, Yue C, Wang D, Qi Z, Tu Y, et al. FoxR2 promotes glioma proliferation by suppression of the p27 pathway. Oncotarget. 2017;8:56255-66.
41. Wander SA, Zhao D, Slingerland JM. p27: a barometer of signaling deregulation and potential predictor of response to targeted therapies. Clinical cancer research : an official journal of the American Association for Cancer Research. 2011;17:12-8.
42. Prasad SB, Yadav SS, Das M, Modi A, Kumari S, Pandey LK, et al. PI3K/AKT pathway-mediated regulation of p27(Kip1) is associated with cell cycle arrest and apoptosis in cervical cancer. Cellular oncology. 2015;38:215-25.
43. Li X, Kong X, Wang Y, Yang Q. BRCC2 inhibits breast cancer cell growth and metastasis in vitro and in vivo via downregulating AKT pathway. Cell death & disease. 2013;4:e757.
44. Seidel S, Garvalov BK, Acker T. Isolation and culture of primary glioblastoma cells from human tumor specimens. Methods in molecular biology. 2015;1235:263-75.
45. Chen X, Hu W, Xie B, Gao H, Xu C, Chen J. Downregulation of SCAI enhances glioma cell invasion and stem cell like phenotype by activating Wnt/beta-catenin signaling. Biochemical and biophysical research communications. 2014;448:206-11.
46. Masilamani AP, Ferrarese R, Kling E, Thudi NK, Kim H, Scholtens DM, et al. KLF6 depletion promotes NF-kappaB signaling in glioblastoma. Oncogene. 2017;36:3562-75.